"NOTICE: When Government or other drawings, specifications or other data are used for any purpose other than in connection with a definitely related Government procurement operation, the U.S. Government thereby incurs no responsibility, nor any obligation whatsoever; and the fact that the Government may have formulated furnished, or in any way supplied the said drawings, specifications or other data is not to be regarded by implication or otherwise as in any manner licensing the holder or any other person or corporation, or conveying any rights or permission to manufacture, use or sell any patented invention that may in any way be related thereto

MANUALS – CORPS OF ENGINEERS
U. S. ARMY

EM 1110-345-432
1 JAN 61

ENGINEERING AND DESIGN

DESIGN OF UNDERGROUND INSTALLATIONS IN ROCK

TUNNELS AND LININGS

ENGINEERING AND DESIGN

DESIGN OF UNDERGROUND INSTALLATIONS IN ROCK

TUNNELS AND LININGS

TABLE OF CONTENTS

LIST OF SYMBOLS

a	Radius of hole
a	Shorter lateral dimension
A	Constant
A_1	Elastic longitudinal incident wave displacement amplitude
A_2	Elastic longitudinal reflected wave displacement amplitude
A_3	Elastic shear reflected wave displacement amplitude
A_4	Elastic longitudinal refracted wave displacement amplitude
A_5	Elastic shear refracted wave displacement amplitude
b	Longer lateral dimension
B	Constant
$c_{a,b}$	Velocity of propagation of longitudinal wave in mediums "a" and "b"
C	Maximum stress concentration around single opening
C_p	Compressive strength of pillar
D	Diameter
D_{max}	Maximum deflection in beam or plate
D_1	Deflection before widening
D_2	Deflection after widening
E	Young's modulus
E_n	Young's modulus of the n^{th} beam
f	Frequency of vibration
F	Safety factor
F_c	Safety factor in compression
F_t	Safety factor in tension
H	Height

k	Multiplying factor
$k\sigma_t$	Maximum amplitude of incident stress pulse
K	Maximum stress concentration in pillars
L	Length, length of span
L	Pulse length
L_1	Span width before widening
L_2	Span width after widening
M	Ratio of S_h/S_v or $\frac{\mu}{1-\mu}$
n	Number of layers formed in spalling process
p, q, r	Parameters for opening shape
r	Radial distance from center of hole, polar coordinate
R	Percent recovery
S_h	Horizontal applied stress
S_v	Vertical applied stress
S_x	Applied stress in x direction, horizontal
S_y	Applied stress in y direction, horizontal
$\bar{S}_b$	Average stress before mining
$\bar{S}_p$	Average pillar stress
t	Thickness of slab
t_n	Thickness of n^{th} beam
T	Tensile strength of rock
T	Tunnel diameter
v	Particle velocity
$v_{a,b}$	Velocity of propagation of shear wave in mediums "a" and "b"
v_1	Velocity of first spall
v_2	Velocity of second spall

W	Weight, lb
w	Width
W_o	Width of opening
W_p	Width of pillar
$W^{1/3}$	Cube root of weight of explosive charge
x, y	Rectangular coordinates
y	Vertical distance from surface
α_1	Incident angle of wave A_1
α_2	Angle of reflection of wave A_1
α_4	Angle of reflection of wave A_4
β	Angle
β_3	Angle of reflection of wave A_3
β_5	Angle of reflection of wave A_5
θ	Angle, polar coordinate
μ	Poisson's ratio
ρ	Density of rock
ρ_a	Apparent density of lowest beam
ρ_b, ρ_a	Density of mediums "b" and "a"
"ρc"	Mechanical impedance of the medium
ρ_n	Density of n^{th} beam
σ_c	Normal stress in the concrete medium due to refraction of stress wave
σ_g	Normal stress in granite before the stress pulse strikes the interface
σ_m	The tensile strength of metal
σ_n	Normal stress in medium "a" before pulse strikes a boundary

σ_{na}	Normal stress in medium "a" after pulse strikes a boundary
σ_{nb}	Normal stress in medium "b" after pulse strikes a boundary
σ_o	The peak compressive stress of the incident wave
σ_r	Radial stress
σ_t	Boundary tangential stress
σ_θ	Tangential stress
τ_{max}	Maximum shear stress
$\tau_{r\theta}$	Shear stress

ENGINEERING AND DESIGN

DESIGN OF UNDERGROUND INSTALLATIONS IN ROCK

TUNNELS AND LININGS

INTRODUCTION

2-01 PURPOSE AND SCOPE. This manual is one of a series issued for the guidance of engineers in the design of underground installations in rock. It is applicable to all elements of the Corps of Engineers who may be concerned with the design and construction of underground military installations. Criteria are presented herein, and in the related manuals of this series, relative to the protection against weapons of modern warfare afforded by underground installations in rock. The physical and economic factors involved in new construction or the conditioning of existing mines for storage purposes and occupancy are discussed. Guidelines have been included relative to devices and measures that should be taken to meet protective requirements.

2-02 REFERENCES. Manuals - Corps of Engineers - Engineering and Design, containing interrelated subject matter are listed as follows:

DESIGN OF UNDERGROUND INSTALLATIONS IN ROCK

EM 1110-345-431 General Planning Considerations
EM 1110-345-432 Tunnels and Linings
EM 1110-345-433 Space Layouts and Excavation Methods
EM 1110-345-434 Penetration and Explosion Effects (CONFIDENTIAL)
EM 1110-345-435 Protective Features and Utilities

a. References to Material in Other Manuals of This Series. In the text of this manual references are made to paragraphs, figures, equations, and tables in the other manuals of this series in accordance with the number designations as they appear in these manuals. The first part of the designation which precedes either a dash, or a decimal point, identifies a particular manual in the series as shown in the table following.

EM	paragraph	figure	equation	table
1110-345-431	1-	1.	(1.)	1.
1110-345-432	2-	2.	(2.)	2.
1110-345-433	3-	3.	(3.)	3.
1110-345-434	4-	4.	(4.)	4.
1110-345-435	5-	5.	(5.)	5.

b. Bibliography. A bibliography is given at the end of each manual in the series. Items in the bibliography are referenced in the text by numbers inclosed in brackets.

c. List of Symbols. Definitions of the symbols used throughout this manual are given in a list following the table of contents.

2-03 RESCISSIONS. This manual is a reissue of material contained in an Engineering Manual on Design of Underground Installations in Rock (13 chapters), dated March 1957, prepared for the Corps of Engineers, U. S. Army, by Bureau of Mines, U. S. Department of Interior.

2-04 MANUAL PREPARATION. The manuals of this series were developed through collaboration of a number of organizations. The Corps of Engineers, U. S. Army, initiated the work and outlined the scope of the manual. Data from the underground explosion test program, underground site surveys, and information grined in the Fort Ritchie project and other construction were furnished to the Bureau of Mines, Department of the Interior, who assumed the responsibility of compiling the manuals. They, in turn, contracted for preparation of certain material by organizations having special competence in the various fields covered. The work of preparation was as follows:

EM 1110-345-431 General Planning Considerations. Prepared by Missouri School of Mines and Bureau of Mines, U. S. Department of Interior.

EM 1110-345-432 Tunnels and Linings. Prepared by the Bureau of Mines, U. S. Department of Interior; and the Rensselaer Polytechnic Institute.

EM 1110-345-433 Space Layouts and Excavation Methods. Prepared by E. J. Longyear Company, Minneapolis, Minnesota.

EM 1110-345-434 Penetration and Explosion Effects (CONFIDENTIAL). Engineer Research Associates.

EM 1110-345-435 Protective Features and Utilities. Prepared by Lehigh University; Bureau of Mines, U. S. Department of Interior; and the Corps of Engineers, U. S. Army

2-05 GENERAL. All underground rock, as a result of nature, is in a state of stress, and any opening created in this rock produces additional stresses in the rock surrounding the opening. Whether or not the opening is stable depends upon the strength of the rock in situ and the magnitude of stresses around the opening. Before designing underground installations for protection against bombing it is first necessary to design underground openings which are stable under the static stresses in the surrounding rock. In this manual paragraphs 2-06 through 2-29 consider the design of underground opening for static stability only, and the design problems considered are restricted to those rock types which are capable of sustaining openings without support. Lined structures which are capable of sustaining both static and dynamic forces with the use of artificial support such as linings, roof bolts, sets, etc., are discussed in paragraphs 2-30 through 2-50.

Mine design has been based generally upon experience and trial-and-error methods. In recent years a more quantitative approach to mine design problems, based upon stress theory, has been used with considerable success. The factors that limit this quantitative approach are the irregularity of the boundaries of the openings, the complexity of the system of openings, the heterogeneity of the rock, a lack of knowledge of the strength of the in-situ rock, and a lack of knowledge of the state of stress in the rock prior to mining. However, by making reasonable assumptions, approximate solutions to various mine design problems have been obtained. Numerous investigators during the last twenty years have contributed to the development of the quantitative approach to mine design problems. Examples of the type of problems considered and the solutions obtained by many of these investigators can be found in references [1, 2, 3, 4, 5, 10, 16, 19, 23, 24, 25] given in the bibliography at the end of this manual. These references cover most of the design problems considered in the manual.

The Applied Physics Laboratory, Bureau of Mines, U. S. Department of the Interior, has been active in the field of underground mine design for many years and has had opportunities to apply quantitative methods to mine structure problems. Theoretical mine designs are checked in the field by

experimental room techniques, as described in reference [15]. The mine design methods presented in this manual have been used in practice at one time or another, and found to give reasonable results.

ASSUMPTIONS USED IN TUNNEL DESIGN

2-06 NECESSITY FOR ASSUMPTIONS AND SAFETY FACTORS. Because the problem of designing safe and stable underground installations is complicated by many factors, simplifying assumptions regarding the openings, rock properties, state of stress, and criteria of failure, are necessary. These assumed conditions are only approximated by openings in rock; therefore, large safety factors in all design equations are required.

2-07 ASSUMPTIONS REGARDING OPENINGS. The opening or system of openings is assumed to be in an infinite medium--a condition that is justified when the distance between the system of openings and the exterior boundary of the medium is greater than three times the size of the openings.

The openings are assumed to be simple geometric shapes, that is, openings having nearly equal dimensions, such as stopes, are represented by spheres or oblate and prolate spheroids. The cross-sectional shapes of adits, drifts, shafts, tunnels, crosscuts, etc., which are long compared to their cross-sectional dimensions, are represented by circles, ellipses, ovaloids, and rectangles with rounded corners.

2-08 ASSUMPTIONS REGARDING THE ROCK FORMATIONS. To simplify design problems, three general types of mediums are considered which are designated as follows: (1) isotropic, homogeneous, (2) horizontal bedded, and (3) inclined bedded formations. In all three of the above types of formations, the rock is assumed to be relatively free from mechanical defects such as open jointing, fractures, etc. When such defects exist, their effect on the stability of the opening can be estimated only by experimental mining, trial-and-error methods of mining, and from previous experience.

a. Isotropic, Homogeneous. Many rock formations have relatively uniform physical properties over large areas and in all directions; therefore, they approach the conditions of an isotropic, homogeneous medium.

Typical examples are massive intrusives such as granite or diorite, massive extrusives such as basalt or rhyolite, some massive metamorphic rocks, and thick bedded sedimentary formations. For the latter group the bed thickness must be large compared to the shorter dimensions of the opening and the bedding planes must be parallel to the length of the opening. For these formations, the stresses around openings may be estimated by elastic theory.

b. Horizontal Bedded. Horizontal bedded formations may be any of the stratified sedimentary rocks where the bed thicknesses are small compared to the shorter cross-sectional dimension of the openings, the bedding planes are parallel to the length of the openings, and the dip is less than 10 percent. These types of formations form several thin beds of rock overlying the opening and the stresses developed in these overlying beds can be estimated by beam or plate theory.

c. Inclined Bedded. Inclined bedded formations are similar to the horizontal bedded formation except that the dip of the beds is greater than 10 percent.

2-09 ASSUMPTIONS REGARDING THE STATE OF STRESS PRIOR TO EXCAVATION. The vertical stress on a unit horizontal section through a mass of rock is equal to the weight of rock above this section, that is

$$S_v = \rho y \qquad (2.1)$$

where

S_v = vertical applied stress

ρ = density of rock

y = vertical distance from surface

The horizontal stress on a vertical section through a mass of rock may vary over wide limits depending upon the geologic history of the rock and the proximity of free vertical boundaries. In an undisturbed mass of rock the horizontal stress at any given point is probably considerably less than the vertical stress. The horizontal stress resulting from vertical loading and horizontal confinement, is related to the vertical stress as Poisson's ratio [16].

$$S_h = \frac{\mu}{1 - \mu} S_v = MS_v \qquad (2.2)$$

where

S_h = horizontal applied stress

S_v = vertical applied stress

μ = Poisson's ratio of the rock

$M = \frac{\mu}{1 - \mu}$

For Poisson's ratio of 1/4, the value of M is 1/3. In a mass of rock which has been disturbed by geologic forces, the horizontal stress depends primarily upon those forces which produce the disturbance. If these forces have disappeared, the horizontal stress in the rock may approach that of undisturbed rock, whereas, if the geologic forces are still active, the horizontal stresses may exceed the vertical stress and approach the compressive strength of the rock.

Three types of stress fields will be considered in this manual. These are represented graphically in figure 2.1 and are given algebraically by equations (2.1) and (2.2) where the value of M is 0, 1/3, or 1. The state of stress represented by M = 0 would be expected to occur at shallow depths near vertical free surfaces. The state of stress represented by M = 1/3 would be expected to occur in undisturbed rock over wide ranges of depth, and that represented by M = 1 could occur at great depth or in folded areas. These three types of stress fields are also assumed to be uniform both along and around the opening. The height of the opening is assumed small compared to the depth below the surface so that variations of stress field with depth in the vicinity of the opening can be neglected. This last assumption has been shown to be valid in a gravity stress field when the depth below the surface

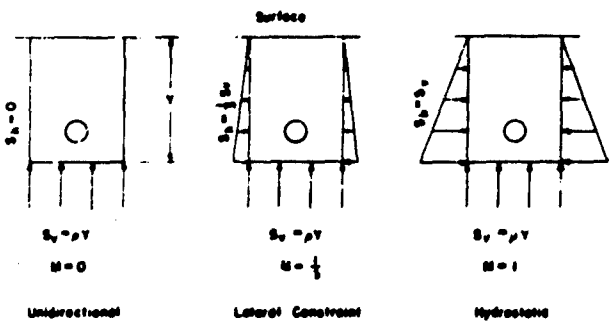

Figure 2.1. Three assumed types of stress fields

is greater than three times the height of the opening [16].

2-10 ASSUMPTIONS REGARDING FAILURE. The criterion of failure assumed for design purposes in this manual is based on maximum stress theory; that is, the rock will fail in tension when the tensile stress exceeds the tensile strength of the rock as determined by a simple flexure test on a sample of the rock. If the tensile stress in the rock is small, the rock will fail in shear at a value of compressive stress equal to the compressive strength of the rock as determined by a simple compression test on a sample of the rock.

2-11 PHYSICAL PROPERTIES. Designing underground openings prior to mining presupposes that samples of the rock (usually in the form of drill core) are available for inspection and physical property determinations. Inspection of drill core or the photographing of the interior of drill holes determines the rock type and the presence of mechanical defects, both of which should be mapped for the area by using core from several holes. Standard physical property tests [16] should be made on core from all drill holes for each rock type encountered. These data should be summarized by rock type giving average values and the normal spread in the data. The most important physical properties for design purposes are density, Young's modulus, compressive strength, and flexural strength. A tabulation of the physical properties for some 200 different rock types from various mining properties throughout the country can be found in references [27] and [28].

2-12 SAFETY FACTORS. The wide variety of assumptions necessary for achieving solutions to design of underground installations requires the use of a liberal factor of safety in design equations. Experience has shown that safety factors of four or more are on the conservative side and are sufficient to allow for most indeterminate variables in mine design problems. Therefore, the following safety factors are recommended: for pillars and sidewalls a safety factor of 4 should be used, and for roof slabs and arches a safety factor between 4 and 8 should be used. Where conditions are such that safety factors of this order of magnitude cannot be used, it is recommended that various instrumentation techniques be used to aid in the detection of failure. For example, the microseismic method of predicting rock failure [17] or extensometers for measuring roof

sag [15] should be employed during the early development stages of mining to check the accuracy of the design methods.

HOMOGENEOUS AND ISOTROPIC FORMATIONS

2-13 GENERAL CONSIDERATIONS. The major problem of designing safe and stable underground openings in massive homogeneous, isotropic rock formations is one of determining the maximum stresses developed in the vicinity of the openings. These maximum stresses, known as critical stresses, must be of smaller magnitude than the ultimate strength of the rock if the opening is to be stable and remain open without the use of artificial support. The maximum stresses developed in the vicinity of openings in homogeneous isotropic formations are a function of opening shape but are independent of opening size. However, infinitely large openings cannot be made in any rock formation because of the presence of mechanical defects. Therefore, the ultimate safe size of any opening is limited by the structural defects found in the rock. Since these defects cannot be evaluated accurately until the opening is formed, only experimental mining techniques and prior experience can be used to determine maximum safe sizes for openings in homogeneous isotropic formations.

For design purposes, underground openings are classified into three general types: single, multiple, and interconnected. The determination of stresses around single openings is the simplest and is discussed first. Stress determinations around systems of multiple openings separated by rib pillars have been made both analytically and photoelastically and are discussed second. No theoretical or experimental work on stress determinations around systems of interconnected openings has been done; therefore, this problem is discussed only briefly.

Stress concentrations around oblate spheroidal-shaped cavities have been found to be lower (approximately 30 percent) than those for infinitely long openings having the same cross section [25]. Thus, for design purposes, only openings that are long compared to their cross section are considered. In addition, if the stress distribution along the length of the opening is assumed to be uniform and independent of the length, the

problem of determining stress distribution reduces to one of plane strain and may be solved as a hole in a wide plate subjected to a two-directional stress field in the plane of the plate.

2-14 SINGLE OPENINGS. a. Circular Tunnels. The stresses induced around a circular hole infinitely far from the boundaries of a plate subjected to a uniform two-directional stress field are given by [26]:

$$\sigma_r = \left(\frac{S_h + S_v}{2}\right)\left(1 - \frac{a^2}{r^2}\right) + \left(\frac{S_h - S_v}{2}\right)\left(1 - \frac{4a^2}{r^2} + \frac{3a^4}{r^4}\right)\cos 2\theta \qquad (2.3)$$

$$\sigma_\theta = \left(\frac{S_h + S_v}{2}\right)\left(1 + \frac{a^2}{r^2}\right) - \left(\frac{S_h - S_v}{2}\right)\left(1 + \frac{3a^4}{r^4}\right)\cos 2\theta \qquad (2.4)$$

$$\tau_{r\theta} = \left(\frac{S_h - S_v}{2}\right)\left(1 + \frac{2a^2}{r^2} - \frac{3a^4}{r^4}\right)\sin 2\theta \qquad (2.5)$$

where

σ_r = radial stress
σ_θ = tangential stress
$\tau_{r\theta}$ = shear stress
a = hole radius
r = radial distance from center of hole
θ = polar coordinate. Horizontal axis represents $\theta = 0$
S_v = vertical applied stress
$S_h = MS_v$ = horizontal applied stress

It is evident from the above relations that the stresses are concentrated near the boundary of the opening, independent of the modulus of elasticity of the material, and independent of the size of the hole, which enters only in the dimensionless ratio (a/r).

For convenience, stresses in the vicinity of an opening are usually expressed as a multiple of the average stress existing outside the zone of disturbance, commonly termed the stress concentration.

Stress concentrations along the major axis at finite distances from a circular opening in a unidirectional stress field, $M = 0$, have been calculated from equations (2.3), (2.4), and (2.5), and are shown in

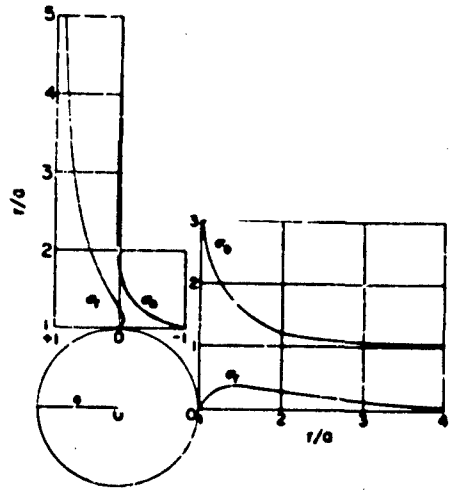

Figure 2.2. Stress concentration along axes of symmetry for circular tunnel, unidirectional stress field

figure 2.2. Since the stresses on or near the free boundary determine whether or not the opening will fail, boundary stresses are considered critical. Figure 2.2 shows that tangential stresses are a maximum at the boundary while radial stresses are zero. The maximum shear stress also occurs at the boundary and equals one-half the tangential stress. For other shaped openings maximum stresses also occur at the boundary; hence only boundary tangential stresses are considered critical.

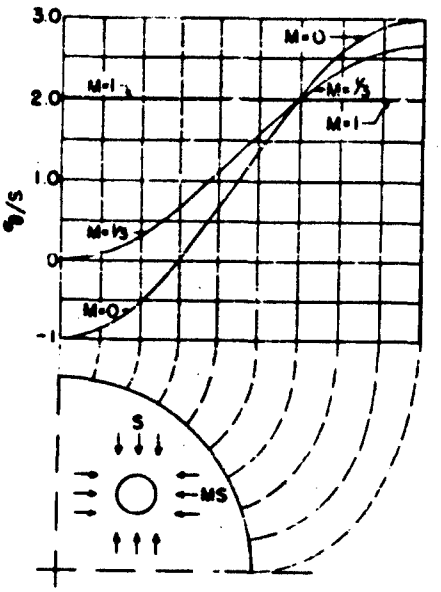

Figure 2.3. Boundary stress concentration for circular tunnels

Figure 2.3 shows the tangential stress distribution around the boundary of a circular opening for the three types of stress fields, $M = 0)$, $M = 1/3$, and $M = 1$.

b. <u>Elliptical Tunnels.</u> The parametric equations

$$x = p \cos \beta; \; y = q \sin \beta \qquad (2.6)$$

define an elliptical opening. The boundary tangential stresses for an elliptical opening in an infinitely wide place subjected to a uniform two-directional stress field are [6]:

$$\sigma_t = \frac{(S_x - S_y)\left[(p + q)^2 \sin^2 \beta - q^2\right] + 2pS_y}{(p^2 - q^2)\sin^2 \beta + q^2} \qquad (2.7)$$

where

σ_t = boundary tangential stress
S_x = applied stress in x direction, horizontal
S_y = applied stress in y direction, vertical
p, q = parameters for ellipse
β = angle
x, y = rectangular coordinates

Equation (2.7) has been used to calculate the boundary stresses around ellipses for four width-to-height ratios (W/H = 0.25, W/H = 0.5, W/H = 2.0, W/H = 4.0) and three types of applied stress fields (M = 0, M = 1/3, and M = 1). The results of these calculations are shown in figure 2.4.

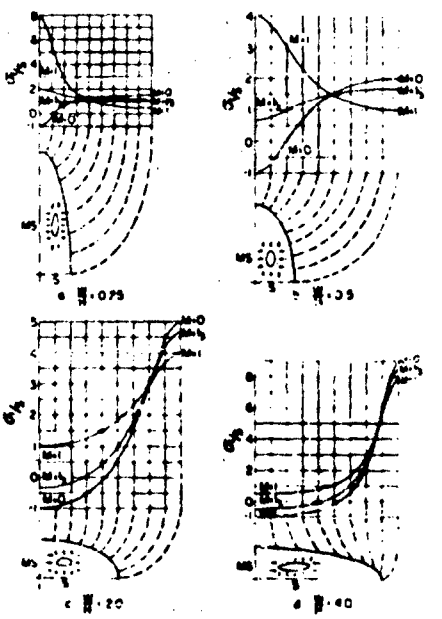

Figure 2.4. Boundary stress concentration for elliptical tunnels

For the unidirectional stress field the maximum stress concentration at the end of the horizontal axis increases as the width-to-height ratio increases, whereas the stress concentration at the top and bottom of the opening remains constant at a value of minus one, signifying tension when the applied stress is compression. For the two-directional stress field (M = 1/3) the boundary stress concentration at the end of the horizontal axis increases with increase in width-to-height ratio, and the stress concentration at the end of the vertical axis changes from large positive values to small negative values. The hydrostatic stress field produces maximum stresses on the horizontal axis for width-to-height ratios greater than one, and on the vertical axis for width-to-height ratios less than one.

c. Ovaloidal Tunnels. An exact solution has been obtained for the stress distribution around an opening in an infinitely wide plate subjected to a two-directional stress field, where the shape of the opening is given by the following parametric equations:

$$x = p \cos \beta + r \cos 3\beta, \quad y = q \sin \beta - r \sin 3\beta \tag{2.8}$$

By selecting proper values for p, q, and r, various shaped openings can be obtained. The boundary stresses for these openings are given by [6]

$$[(p^2 + 6rq) \sin^2 \beta + (q^2 + 6rp) \cos^2 \beta - 6r (p + q) \cos^2 2\beta + 9r^2] \sigma_t$$
$$= (S_x + S_y) (p^2 \sin^2 \beta + q^2 \cos^2 \beta - 9r^2)$$
$$- \frac{(p^2 - q^2) (S_x + S_y) - (p + q)^2 (S_x - S_y)}{p + q - 2r} [(p - 3r) \sin^2 \beta$$
$$- (q - 3r) \cos^2 \beta] \tag{2.9}$$

where

σ_t = tangential boundary stress
S_x = applied stress in x direction, horizontal
S_y = applied stress in y direction, vertical
p, q, r = parameters for opening shape
β = angle
x, y = rectangular coordinates

Using the values of p, q, and r given in table 2.1, four different shaped openings resembling ovaloids, i.e. rectangles with semicircular ends, were constructed from equation (2.8). The boundary stresses

Table 2.1. Values of Parameters for Approximate Ovaloids

Width-to-Height Ratio	p	q	r
0.25	1.19	4.19	-0.19
0.50	1.1	2.1	-0.1
2.0	2.1	1.1	-0.1
4.0	4.19	1.19	-0.19

around these ovaloidal shapes were calculated from equation (2.9) for the three types of stress fields and the results are given in figure 2.5.

The maximum boundary stresses around approximate ovaloidal openings do not occur on the axis of the opening as in the case of elliptical openings, but are shifted toward the junction of the semicircular end and the straight sides. Otherwise, the boundary stresses around ovaloidal openings are similar to those for elliptical openings.

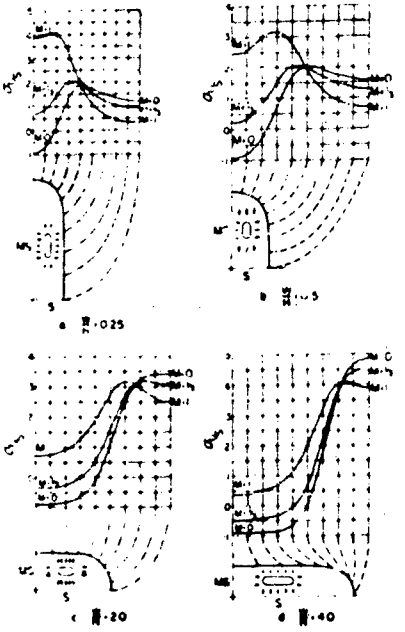

Figure 2.5. Boundary stress concentration for ovaloidal tunnels

d. Rectangular Tunnels. The tangential stress distribution around a rectangular opening with rounded corners has been studied by the photoelastic method [4, 19]. Rounded, i.e. filleted, corners were used to avoid extremely high corner stresses. The boundary stresses around five different rectangles with constant ratio of fillet radius to short dimension are shown for three types of stress fields in figure 2.6.

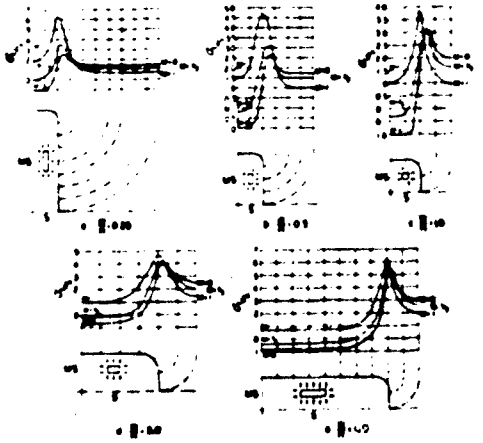

Figure 2.6. Boundary stress concentration for rectangular tunnels with rounded corners. Ratio of fillet radius to short dimension = 1/6

The maximum stress concentration occurs at the corners for all cases. For M = 0 , the stress concentration increases with increase of W/H. For M = 1/3 or 1 , the stress concentration at the corners is a minimum for W/H = 1. When M = 0 or 1/3 , there is a tensile stress

induced in the roof, but in the hydrostatic field, M = 1 , no tensile stresses are induced.

2-15 DESIGN PRINCIPLES, SINGLE OPENINGS. a. Discussion. The results of the preceding sections are summarized into a set of critical stress curves for use in designing single openings in homogeneous isotropic rock formations. Figures 2.7, 2.8, 2.9, and 2.10 show the variation of critical compressive and tensile stresses versus W/H for elliptical, ovaloidal, and rectangular openings in plates for the three types of applied stress fields. The curves in these figures are used to estimate the critical stresses for various shaped openings in different types of stress fields. Also, the following set of design principles can be obtained from the above data.

b. List of Principles. (1) If subsurface conditions approximate those of the unidirectional stress field acting vertically, an elliptical-shaped opening with the major axis vertical gives the smallest critical stress. Furthermore, the greater the ratio of major to minor axis, the lower will be the critical stress. However, if an opening is required whose width-to-height ratio is greater than unity, either an ovaloid or a rectangle with rounded corners is a better choice than an ellipse.

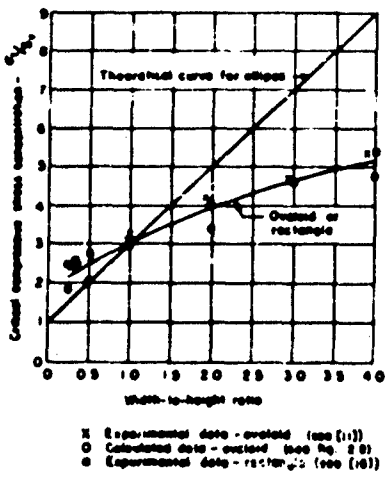

Figure 2.7. Critical compressive stress concentration for tunnels of various cross sections, unidirectional stress field. $S_h = S_v$, $S_v = 0$

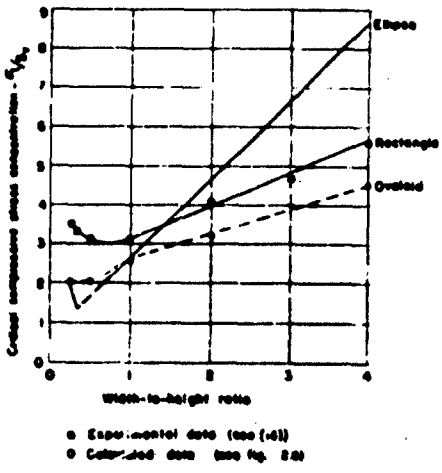

Figure 2.8. Critical compressive stress concentration for tunnels of various cross sections, two-directional stress field. $S_h = 1/3\, S_v$

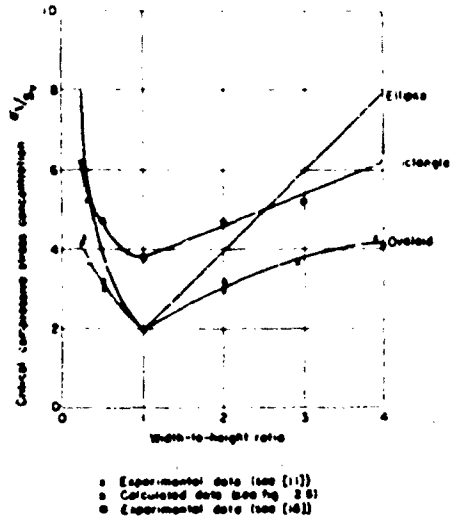

Figure 2.9. Critical compressive stress concentration for tunnels of various cross sections, hydrostatic stress field. $S_h = S_v$

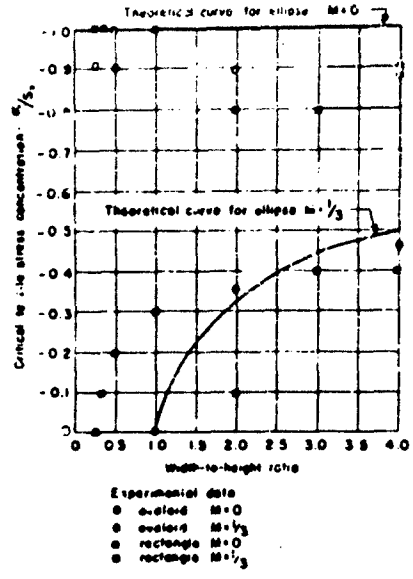

Figure 2.10. Critical tensile stress concentration for tunnels of various cross sections, two types of stress fields. M = 0, M = 1/3

(2) Under the action of a unidirectional vertical stress field, there is developed in the roof a stress concentration of approximately -1, i.e., the stress in the roof is in tension and is equal to the applied compressive stress. Since the tensile strength of most rock is usually very low compared to its compressive strength, this tension may be critical.

(3) When there is a two-directional stress field, and M equals approximately 1/3, an elliptical or ovaloidal opening with major axis vertical induces lower critical stresses than the rectangle. Moreover, the critical stress becomes a minimum when the ratio of major to minor axis is about 1/3. If the ratio of width to height of the opening is greater than unity, ovaloidal or rectangular openings induce lower critical stresses than elliptical openings.

(4) In a two-directional stress field when $M = 1/3$, roof tensions are induced only when the width-to-height ratio of the opening is greater than unity. Although the tensile stress concentration is lower at all times than for a unidirectional vertical stress field, the magnitude of the stress increases with increase of width-to-height ratio, and

is virtually independent of opening shape.

(5) In a hydrostatic stress field, the preferred opening shape is a circle. When a width-to-height ratio either small or greater than unity is desired, an ovaloid will induce lower critical stresses than either the ellipse or rectangle.

(6) In a hydrostatic stress field no tensile stresses are induced for any of the opening shapes.

(7) Sharp corners or an opening in any type of stress field will produce high stress concentrations, and should be avoided.

2-16 ILLUSTRATIVE EXAMPLE, SINGLE OPENING. Determine the safety factors that exist for the stresses around a long rectangular opening 25 ft wide and 10 ft high at a depth of 900 ft in the center of a uniform sandstone bed 70 ft thick, having the following physical properties:

Compressive strength = 18,000 psi
Modulus of rupture = 1,600 psi
Poisson's ratio = 0.25
Rock density = 0.09 lb per cu in.

Rounded corners for the opening will be assumed since routine blasting rarely produces sharp corners. The stress field prior to mining may be assumed to result only from the weight of superincumbent rock and lateral confinement. Therefore, from equations (2.1) and (2.2):

$$\text{Vertical stress} = S_v = \rho z = 0.09 \times 900 \times 12 = 970 \text{ psi}$$

$$\text{Value of } M = M = \frac{\mu}{1-\mu} = \frac{0.25}{1-0.25} = 1/3$$

$$\text{Horizontal stress} = S_h = MS_v = 1/3 \times 970 = 320 \text{ psi}$$

The width-to-height ratio for the rectangular opening is 2.5; therefore, from figure 2.8 the maximum compressive stress concentration in the sidewalls is 4.4 and from figure 2.10 the maximum tensile stress concentration in the roof is 0.4. Hence, the critical stresses on the boundary are:

Critical compressive stress = 970 × 4.4 = 4300 psi
Critical tensile stress = 970 × 0.4 = 390 psi

The safety factors are the ratio of compressive strength to maximum compressive stress, and the ratio of modulus of rupture to maximum tensile stress: Thus

$$F_c = \frac{18,000}{4,300} = 4.2; \quad F_t = \frac{1,600}{390} = 4.1$$

Since both safety factors exceed 4, which has been taken as a normal safety factor, the opening should be stable under the assumed operating conditions.

2-17 MULTIPLE OPENINGS IN HOMOGENEOUS AND ISOTROPIC FORMATIONS.

a. Stress Distribution. The stress distributions around systems of parallel openings separated by rib pillars is considerably more complicated than for a single opening. Therefore, this problem is discussed only briefly and the design methods are based upon empirical results rather than theoretical equations. The boundary stress distribution for a row of equally spaced holes of equal size in a plate subjected to a unidirectional compressive stress field perpendicular to the line of holes has been determined analytically for circular openings [11] and photoelastically for circular, ovaloidal, and rectangular openings [5, 19]. Irrespective of the number or shape of the openings, the following generalizations regarding the stress distribution around the system of openings can be made. First, the maximum boundary compressive stresses occur on the sidewalls of the openings, that is, along the edge of the pillars between the openings. For a finite number of openings the boundary stress concentration is greatest for the innermost holes and approaches the maximum value of the stress concentration for an infinite number of openings. Second, the boundary stress at the top and bottom of the openings is tension and is approximately equal in magnitude to the applied compressive stress. However, this tensile stress concentration decreases rapidly with applied confining pressures. Third, the pillar stress concentration increases as the opening-to-pillar width ratio increases, but the stress distribution through the pillar becomes more uniform. Thus, when the pillar width is small compared to the opening width, the average stress in the pillar is nearly equal to the maximum stress.

b. Unidirectional Stress Field. The following equation has been derived from experimental data [5]

$$K = C + 0.09 \left[\left(1 + \frac{W_o}{W_p} \right)^2 - 1 \right] \qquad (2.10)$$

where

K = maximum stress concentration in pillars

C = maximum stress concentration around a single opening for unidirectional stress field

W_o = width of opening

W_p = width of pillar

By use of equation (2.10), the maximum stress concentration in rib pillars for a series of parallel openings can be computed from the ratio of opening width to pillar width and the maximum stress concentration around a single opening of the same shape. Various values of C for use in equation (2.10) for different shaped openings may be obtained from the curves given in figure 2.7. Equation (2.10) has been evaluated for circles, ovaloids, and rectangles and the corresponding maximum stress concentration in the pillars as a function of opening width to pillar width is shown in figure 2.11 together with available experimental data. Also shown in figure 2.11 is the average pillar stress concentration as a function of opening-to-pillar width. This average pillar stress is obtained by assuming that the pillars uniformly support the entire load of the overlying rock.

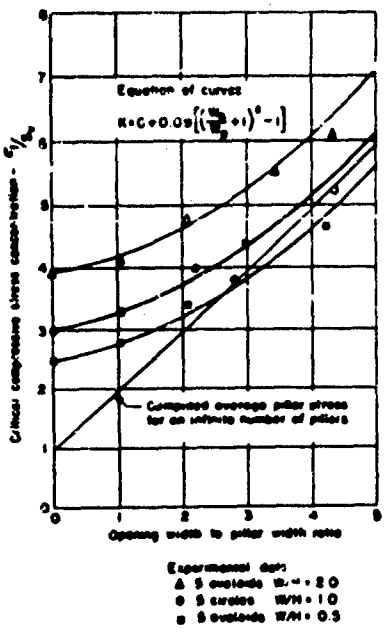

Figure 2.11. Critical compressive stress concentration for multiple openings

c. Two-Directional Stress Fields.

Analytical studies on the stress distribution around multiple openings for two-directional applied stress fields are inadequate for obtaining design criteria. However, by combining the results for single openings in two-directional stress fields with those for multiple openings in unidirectional stress fields an approximate design method can be obtained. Thus, it is assumed that equation (2.10) can be used for two-directional stress fields by simply using for C the value of the critical stress concentration around a single opening in a two-directional stress field (figures 2.8 and 2.9)

instead of the value for the unidirectional stress field.

2-18 ILLUSTRATIVE EXAMPLE, MULTIPLE OPENING. Determine if a row of 30-ft-diameter circular tunnels can safely be spaced on 60-ft centers at a depth of 1000 ft in a homogeneous isotropic rock formation having the following physical properties:

Density = 0.095 lb per cu in.
Compressive strength = 15,000 psi
Modulus of rupture = 800 psi
Poisson's ratio = 0.25

A lateral confining pressure is assumed; therefore, the applied stress field is

$$S_v = 0.095 \times 1000 \times 12 = 1140 \text{ psi}$$

$$S_h = \frac{0.25}{1 - 0.25} \times 1140 = 377 \text{ psi}$$

From figure 2.8 the critical boundary compressive stress concentration is 2.67 for a circular opening and from figure 2.10 the critical tensile stress is zero; therefore, design is based only on compressive stresses. Substituting in equation (2.10) gives

$$K = 2.67 + 0.09 [(1 + 1)^2 - 1] = 2.67 + 0.09 \times 3 = 2.94$$

A stress concentration of 2.94 gives a critical stress of

$$2.94 \times 1140 = 3350 \text{ psi}$$

The ratio of the compressive strength to critical stress is the safety factor, thus

$$\frac{15,000}{3,350} = 4.5$$

Since the safety factor is greater than 4 the above system of openings should be a safe and stable installation in the absence of any abnormal geological defects.

2-19 INTERCONNECTED OPENINGS. The stress distribution for systems of interconnected openings, such as used in room and pillar methods of mining,

has not been studied analytically. The assumed basis for design therefore is either the average pillar stress or the maximum boundary stress for a single opening, whichever is the larger. In general, average pillar stresses for interconnected openings will be larger than maximum boundary stresses for a single opening when the mined area exceeds 75 percent, that is, when the opening-to-pillar width ratio is greater than 1 for square pillars.

Critical or maximum boundary stresses for various shaped single openings have already been given. The method for designing safe pillar support from average stress is given in the next section.

OPENINGS IN HORIZONTAL BEDDED FORMATIONS

2-20 GENERAL CONSIDERATIONS. The design of underground openings in a horizontal bedded formation can be divided into two major problems: first, the determination of safe span lengths, and second, the determination of safe pillar support. Each of these problems can be subdivided according to the system of openings: first, the single opening; second, parallel openings separated by rib pillars; and third, interconnected openings supported by square pillars.

a. Safe Span Length. For single openings, the determination of safe span length is based upon the assumption that the roof slab may be represented either by a uniformly loaded beam fixed at both ends or a uniformly loaded rectangular plate fixed on all edges. Furthermore, it is assumed that: the roof slab extends over the entire opening and has no vertical cracks or fractures, there is no bond between the roof slab and the rock above, the roof slab is a homogeneous, isotropic rock having a linear stress strain relation, and no confining pressures exist at the edges of the slab. The effect on a roof slab of an axial load resulting from confining pressures in the rock has been calculated and found, in practical cases, to contribute less than 10 percent to the bending moments [22]. Therefore, only vertical loads are considered for design purposes. For single openings where the ratio of the lateral dimensions is greater than 2:1, beam theory is used, and less than 2:1, plate theory is used.

The determination of safe span lengths for parallel openings separated by rib pillars presents no additional problems. Each opening is considered independently and either the beam or plate theory is used for calculating safe span lengths depending upon the ratio of room length to width.

The problem of determining safe span lengths for interconnected openings supported by pillars has no known theoretical solution. Therefore, a relatively large safety factor, 8, is employed with the simple beam theory to allow for the additional stresses created by having only partial support at the edges of the slab. The distance between rows of pillars is considered the span length.

b. Safe Pillar Support. The determination of safe pillar support for a single opening reduces to an estimation of the sidewall stresses. These stresses are estimated from the boundary stresses around single openings in homogeneous, isotropic medium.

The determination of safe pillar support for parallel openings separated by rib pillars or interconnected openings with square pillar support is based upon the assumption that the load on underground pillars results only from the weight of the rock above the openings and pillars, and that the loading conditions are similar to those in a simple compression test. The average compressive strength determined by laboratory tests on samples of the pillar rock is assumed to be the average strength of the pillar rock in situ.

2-21 SAFE SPAN LENGTHS IN HORIZONTAL BEDDED FORMATIONS, BEAM THEORY.

a. Single-Layer Roof. The maximum values of the deflection, shear, and tension for a uniformly loaded beam clamped at both ends are given [24]

$$D_{max} = \frac{\rho L^4}{32Et^2} \qquad (2.11)$$

$$\tau_{max} = \frac{3\rho L}{4} \qquad (2.12)$$

$$\sigma_{max} = \frac{\rho L^2}{2t} \qquad (2.13)$$

where

D_{max} = maximum deflection
τ_{max} = maximum shearing stress
σ_{max} = maximum tensile stress
L = span length (shorter lateral dimension slab)
t = slab thickness
E = Young's modulus
ρ = density of rock

The maximum deflection occurs at the center of the beam and the maximum shear and tensile stresses occur at the ends of the beam. At the center of the beam the shear is zero, and the tension is one-half the maximum value, thus, the expected points of initial failure would be at the ends of the span rather than at the center.

The maximum shear stress varies directly as the span length, whereas the maximum tensile stress varies as the square of span length, and inversely as the slab thickness. The ratio of these stresses is:

$$\frac{\sigma_{max}}{\tau_{max}} = \frac{2L}{3t} \tag{2.14}$$

Thus, for beams long compared to their thickness, the tensile stress exceeds the shear stress. Since for most rock the tensile strength is less than the shear strength, shear stresses can be disregarded and only tensile stresses employed to determine safe span lengths.

Equation (2.13) may be rewritten as a design formula for safe span lengths by replacing σ_{max} with T, the tensile strength of the rock dividing T by F, a safety factor; and solving for L. Thus

$$L = \sqrt{\frac{2Tt}{\rho F}} \tag{2.15}$$

Using a safety factor of 8 and a rock density of 0.09 lb per cu in., a graph of equation (2.15) on log-log coordinates is shown in figure 2.12. This graph relates safe span length to bed thickness and tensile strength. Figure 2.12 may be used for rough estimates of safe span length and

equation (2.15) for more precise calculation.

b. Two-Layer Roof. When the roof rock is composed of two slabs, one above the other, there

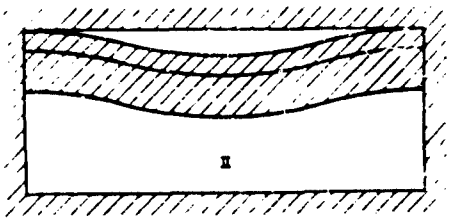

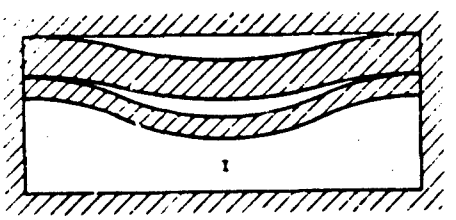

Figure 2.13. Two conditions for multi-layered roof slabs

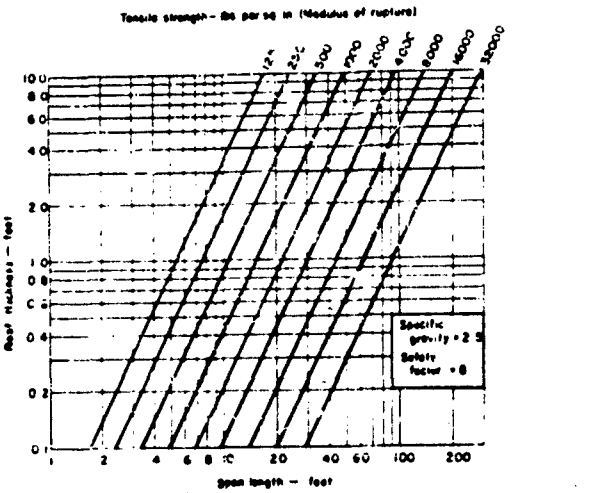

Figure 2.12. Safe span length for various roof thicknesses and tensile strengths of rock

are two cases to consider (see figure 2.13). First, when the thicker slab overlies the thinner slab, each acts independently and the stresses and deflection in each slab can be calculated by equations (2.11), (2.12), and (2.13). Second, when the thinner slab overlies the thicker, the lower slab is loaded by the upper one. This additional loading can be calculated from beam theory and represented as an apparent density of the lower slab which is given by

$$\rho_a = \frac{E_1 t_1^2 (\rho_1 t_1 + \rho_2 t_2)}{E_1 t_1^3 + E_2 t_2^3} \qquad (2.16)$$

where ρ_a = apparent density of lower beam
E_1 = Young's modulus of lower beam
E_2 = Young's modulus of upper beam
ρ_1 = density of lower beam
ρ_2 = density of upper beam
t_1 = thickness of lower beam
t_2 = thickness of upper beam

The maximum values of the deflection, shear, and tensile stress in the lower slab are determined by equations (2.11), (2.12), and (2.13), respectively, where ρ is replaced by ρ_a. If the density and Young's modulus are the same for both slabs, the maximum value of ρ_a occurs when the upper slab is one-half the thickness of the lower. Under this condition $\rho_a = 4/3\ \rho_1$; hence the upper slab increases the tensile stresses in the lower slab by 33-1/3 percent. Safe span lengths for the case of two beams may be determined from equation (2.15) by replacing ρ with ρ_a.

c. Multiple-Layer Roof. When the roof rock is composed of three or more slabs having no bond between slabs and the thinner slabs overlie the thicker ones, the additional load on the lowest slab can be calculated from beam theory and represented as an apparent density of the lowest slab which is given by

$$\rho_a = \frac{E_1 t_1^2 (\rho_1 t_1 + \rho_2 t_2 + \rho_3 t_3 + \ldots + \rho_n t_n}{E_1 t_1^3 + E_2 t_2^3 + E_3 t_3^3 + \ldots + E_n t_n^3} \qquad (2.17)$$

where

ρ_a = apparent density of lowest beam
E_n = Young's modulus of n^{th} beam
ρ_n = density of n^{th} beam
t_n = thickness of n^{th} beam

The values of the maximum deflection, shear, and tensile stress and the safe span length are again obtained by substituting ρ_a for ρ in equations (2.11), (2.12), (2.13), and (2.15), respectively.

For multilayered roof slabs having various thicknesses and physical properties, the number of layers that need to be considered can be determined by using equation (2.17) stepwise. That is, the apparent density is calculated for the first two slabs, then the first three, first four, etc., until the apparent density shows no further increase. Only those layers that produce an increase in the apparent density are effectively loading the lowest layer.

2-22 SAFE SPAN LENGTHS IN HORIZONTAL BEDDED FORMATIONS, PLATE THEORY. The maximum values of the deflection and tensile stress for a uniformly loaded rectangular plate clamped on all edges are given [22]

$$D_{max} = \frac{A\rho a^4}{Et^2} \tag{2.18}$$

$$\sigma_{max} = \frac{6B\rho a^2}{t} \tag{2.19}$$

where

D_{max} = maximum deflection
σ_{max} = maximum tensile stress
a = shorter lateral dimension
b = longer lateral dimension
E = Young's modulus
ρ = density
t = thickness
A, B = constants

Table 2.2. Values of A and B for Various Values of b/a and Poisson's Ratio Equal to 1/3

b/a	B	A
1.0	0.0513	0.0138
1.1	0.0581	0.0164
1.2	0.0639	0.0188
1.3	0.0687	0.0209
1.4	0.0726	0.0226
1.5	0.0757	0.0240
1.6	0.0780	0.0251
1.7	0.0799	0.0260
1.8	0.0812	0.0267
1.9	0.0822	0.0272
2.0	0.0829	0.0277

The maximum deflection occurs at the center of the plate and the maximum tensile stress occurs at the middle of the longer dimension at the edge of the plate. For ratios of b/a greater than 2.0, the beam theory

equations given in paragraph 2-21a approximate the stresses and deflection of the plate theory. The error in the maximum stress is less than 1 percent and the error in the maximum deflection is less than 12 percent.

As before, equation (2.19) can be rewritten as a design formula for safe span length by replacing σ_{max} with T, the tensile strength of the rock; dividing T by a safety factor, F; and solving for a, the shorter lateral dimension. Thus, the safe span length is given by

$$a = \sqrt{\frac{Tt}{6BpF}} \tag{2.20}$$

2-23 ILLUSTRATIVE EXAMPLE, SAFE SPAN LENGTH. The estimation of safe span lengths from equation (2.15) or (2.20) requires values for the safety factor, density, modulus of rupture of the roof rock, and the thickness of the roof slab. When the roof rock is composed of two or more slabs with the upper ones loading the lower ones, then the density and Young's modulus of each slab are also required.

Safety factors between 4 and 8 should be employed, depending upon the type and number of mechanical defects that can be observed in the roof rock. The density, Young's modulus, and modulus of rupture are obtained from physical property tests on diamond-drill core obtained from the roof rock. When available, the modulus of rupture determined on horizontal core should be used, otherwise, vertical core may be used. Prior to mining the opening, the bed thicknesses overlying the opening are estimated by inspecting vertical drill cores of the roof rock and noting planes of weakness. After mining an opening, the estimated bed thicknesses may be checked by stratascope surveys and sag measurements as the original opening is periodically widened. From equation (2.11) the apparent bed thickness can be calculated from the change in deflection resulting from a change in span width which is given by

$$t = \sqrt{\frac{\rho}{32E}\left(\frac{L_2^4 - L_1^4}{D_2 - D_1}\right)} \tag{2.21}$$

where

L_2 = span width after widening
L_1 = span width before widening
$D_2 - D_1$ = sag resulting from widening

A complete discussion of the experimental techniques employed in developing safe span lengths at the Bureau of Mines Oil Shale Mine, Rifle, Colorado, has been reported [15].

As an example illustrative of safe span design, consider the following problem. Determine the maximum safe span for an underground installation in a stratified formation 600 ft below the surface, consisting of a single opening 30 ft high. Inspection and physical property tests on diamond-drill core from the proposed roof rock have given the following data:

	Slab Thickness, ft	Density lb/cu in.	Young's Modulus, psi	Modulus of Rupture, psi
First slab	6	0.09	3×10^6	3×10^3
Second slab	2	0.09	2×10^6	2×10^3
Third slab	10	0.09	3×10^6	3×10^6

The second slab will load the first slab as it is thinner than the bottom slab, but the third slab will not load the bottom slab because it is much thicker than the lower one. To calculate the additional loading on the lower slab use equation (2.16) to obtain the apparent density of the bottom slab. Thus

$$\rho_a = \frac{3 \times 10^6 (6 \times 12)^2 (0.09 \times 6 \times 12 + 0.09 \times 2 \times 12)}{3 \times 10^6 (6 \times 12)^3 + 2 \times 10^6 (2 \times 12)^3} = 0.[illegible] \text{ lb/cu in.}$$

Substituting ρ_a for ρ in equation (2.15) gives the estimated safe span as

$$L = \sqrt{\frac{2 \times 3 \times 10^3 \times 6 \times 12}{0.117 \times 8}} = 56 \text{ ft}$$

2-24 SAFE PILLAR SUPPORT IN HORIZONTAL BEDDED FORMATIONS. a. Single Openings. The determination of safe pillar support for a single opening in a horizontal bedded formation reduces to an estimation of the boundary stresses in the sidewalls. Depending upon the type of stress field and the general shape of the opening, the critical boundary stresses are obtained from the appropriate curves in figures 2.7, 2.8, and 2.9. The critical boundary stresses should always be less than the strength of the rock and preferably by a factor of 4.

b. Parallel Openings. The average stress on rib pillars between a series of equally spaced parallel openings of equal size is given [5]

$$\bar{S}_p = \left(1 + \frac{W_o}{W_p}\right)\bar{S}_b \qquad (2.22)$$

where

$\bar{S}_b$ = ρy = average vertical stress before mining
$\bar{S}_p$ = average stress in pillars
W_o = opening width
W_p = pillar width
ρ = density of rock
y = depth below surface

Equation (2.22) may be rewritten as a design formula for safe pillar widths of rib pillars by replacing $\bar{S}_p$ by C_p, the compressive strength of the pillar; dividing C_p by F, a safety factor; and solving for W_p. Thus, the safe pillar width is given by

$$W_p = \frac{W_o}{\frac{C_p}{F\bar{S}_b} - 1} \qquad (2.23)$$

c. Interconnected Openings. The average stress on square pillars for a system of interconnected openings in a horizontal bedded formation is given [5]

$$\bar{S}_p = \bar{S}_b \left(1 + \frac{W_o}{W_p}\right)^2 \qquad (2.24)$$

where

W_p = width of pillar (same in both lateral directions)
W_o = opening width (same in both lateral directions)
$\bar{S}_p$ = average stress in pillar
$\bar{S}_b$ = average stress before mining

Replacing $\bar{S}_p$ by C, the compressive strength of the pillar; dividing C_p by F, a safety factor; and solving for W_p gives the safe pillar width design formula for square pillar support as

$$W_p = \frac{W_o}{\sqrt{\frac{C_p}{F\bar{S}_b} - 1}} \qquad (2.25)$$

For mining purposes the percent mined area or percent recovery, R, is often useful. Equations (2.23) and (2.25) can be put in terms of safe percent recovery, giving

$$R = 100\left(1 - \frac{F\bar{S}_b}{C_p}\right) \qquad (2.26)$$

2-25 COMPRESSIVE STRENGTH OF PILLARS. The compressive strength of pillars, C_p, used in equations (2.23), (2.25), and (2.26) needs some clarification. Laboratory test on diamond-drill core has shown that the observed compressive strength is a function of the length-to-diameter ratio, L/D, of the sample [12]. Standard compressive tests are performed on samples having an L/D ratio equal to one and the necessary correction for the compressive strength of samples having an L/D ratio between 0.5 and 2.0 amounts to less than ±20 percent. Therefore, no correction for the compressive strength of pillars whose ratio of L/D lies between 0.5 and 2.0 is required. Pillars having L/D ratios greater than 2.0 should be avoided because the "column effect" reduces the strength of the pillar appreciably.

The strength of underground pillars in stratified formations presents some difficulties because the strengths of the various strata of rock in

the pillar vary over wide limits. Unpublished laboratory tests by the Applied Physics Branch have shown that, in general, the strength of pillars composed of different strata of rock is more nearly equal to the average strength of the various strata of rock rather than the weakest strata. Therefore, the compressive strength of pillars in stratified formations should be obtained by averaging the compressive strengths of the various rock types in the pillar.

2-26 ILLUSTRATIVE EXAMPLE, SAFE PILLAR SUPPORT. The estimation of safe pillar widths by means of equations (2.23) and (2.25) required values for compressive strength of pillar, height-to-width ratio of pillar, opening width, safety factor, and average stress before mining. Methods for estimating compressive strength of pillars having various height-to-width ratios composed of stratified rock have been given in the preceding paragraph. A safety factor of at least 4 should be employed and the height-to-width ratio of the pillar should be kept below 2. The opening width is determined from safe span considerations and is assumed fixed. The average stress before mining is given by equation (2.1). For a quick estimate, average vertical stress in rock increases 1 psi per foot of depth.

As an illustrative example consider the following problem. Determine the safe pillar widths for an underground installation in a stratified formation 1000 ft below the surface consisting of 30-ft-high interconnected openings supported by square pillars where the safe opening width or distance between pillars has been fixed at 50 ft. Physical property tests on vertical drill core from the pillar rock have provided the following data:

Strata	Thickness, ft	Average Compressive Strength, psi
1	15	20,000
2	5	10,000
3	10	15,000

The average compressive strength for a pillar having a height-to-width ratio of 1 is the average strength of the three strata or 16,000 psi. The average stress before mining at 1000 ft is approximately 1000 psi.

Assuming a safety factor of and substituting into equation (2.25) gives the safe pillar width as

$$W_p = \frac{50}{\sqrt{\frac{16,000}{4 \times 1,000} - 1}} = \frac{50}{\sqrt{4 - 1}} = 29 \text{ ft}$$

Since the ratio of height to width of pillar is approximately unity, no correction need be made.

INCLINED BEDDED FORMATIONS

2-27 GENERAL. In dipping strata, a tunnel is usually driven parallel to the dip or parallel to the strike. For the purposes considered in this manual, the maximum bedding angle which could be followed is limited to about a 10 percent grade, above which movement of wheeled vehicles and equipment would be hampered. The design problem at such small angles is virtually the same as for horizontal bedded formations, and safe spans may be calculated using the same equations from either beam or plate theory as the case requires. Pillars are designed in exactly the same manner as prescribed for those in horizontal strata. Examination of the forces acting in an inclined roof beam shows that the normal component of the vertical load which tends to flex the beam is less than the total load, and hence, the bending effect is lessened. Thus, the factor of safety is even greater than where the same roof bed lies horizontal.

2-28 TUNNEL PERPENDICULAR TO STRIKE. Openings made across bedded formations which are sharply inclined are not advisable unless artificial supports are used. Since the dip in this case is assumed greater than that which would produce a 10 percent grade in a tunnel driven parallel to the stratification, the tunnel could not be driven inclined and will be considered horizontal. When the long dimension of the opening lies in a horizontal plane which is perpendicular to the direction of the strike of the beds (see figure 2.14), the edges of numerous overlying strata are exposed along the

Figure 2.14. Longitudinal section of horizontal tunnel driven perpendicular to strike of inclined bedded formation

entire length of the tunnel and will tend to crack and drop into the opening. Moreover, in the extreme case where these beds are of widely varying thicknesses and physical properties, the problem of determining span width analytically would be virtually impossible. In any case, all exposed edges of roof beds must be supported by roof bolts or some similar expedient.

2-29 TUNNEL PARALLEL TO STRIKE. When the long dimension of the opening is horizontal and lies parallel to the strike under sharply dipping roof beds, the top of the opening may be made to conform as close as possible to the dip of the beds; see figure 2.15. This would minimize the possibility of differential movement of thin beds into the tunnel, but roof bolts would still be necessary to support exposed edges of strata.

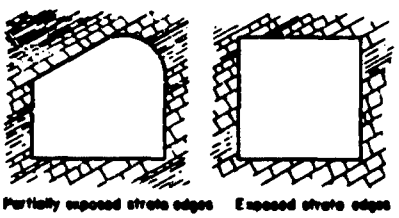

Figure 2.15. Cross sections of horizontal tunnels driven parallel to strike of inclined bedded formation

TUNNEL LININGS TO RESIST EXPLOSIONS

2-30 GENERAL DISCUSSION. A statically stable opening is defined as an underground opening that will successfully resist the static loads imposed by the overlying material. Such an opening may require no supporting means, or may require some artificial support such as roof bolts, linings, or some type of structural framework. One anticipates that in large and/or long openings, defective rock areas will exist where some type of static load support will be required. Before the problem of designing an internal tunnel structure is considered, it is assumed that a statically stable opening can exist with or without artificial supports. Any internal tunnel structure designed for protection against dynamic loadings is distinguished primarily from the usual type of static support by its purpose.

The problems encountered in driving an opening through various media have been described in the preceding paragraphs. The principles discussed are predicated on the assumptions that the tunnels are in a rock medium under conditions that allow it to be considered statically stable with no

additional supports. In the cases where additional supports are required for static stability, these supports may be designed to resist dynamic loads as well, since the principles involved are quite parallel. However, the mode of failure resulting from the dynamic loadings can be quite different.

Linings, when used for static support, may range from a thin coating of mortar such as Gunite, to a thick wall of plain or reinforced concrete of various structural shapes and designs. Structural steel elements are also frequently used. The mechanism of damage as discussed in this manual applies directly in the cases of light tunnel linings, like Gunite, placed to protect against rock spalling and sloughing due to air slaking, since such a thin coat will add no material strength. Also, the use of roof bolts does not materially affect the damage due to dynamic loadings. Heavy supporting structures in direct contact with the tunnel walls experience a major effect from compressive stress pulse loadings, and design of such structures should incorporate the principles for protection from dynamic loadings. Areas requiring special supports are as much of a special problem in design for dynamic loads as they are for static loads. In such cases special static and dynamic design should be considered simultaneously.

2-31 REASONS FOR INTERNAL TUNNEL STRUCTURE. An underground explosion subjects the rock medium to a compressive stress pulse which may cause extensive damage at free surfaces such as the unprotected walls of a tunnel. The extent of the damage that may be generated depends upon the amplitude of the stress pulse, the shape of the stress pulse, and the physical condition of the rock at the surface of the tunnel. Experiments on tunnel damage have been carried out by the Corps of Engineers [6, 7, 8]. These reports define four degrees of damage intensity which will be discussed later. Tunnel damage does not necessarily mean collapse of the tunnel nor impairment of tunnel static stability, but is generally considered to mean breakage of rock at the wall surfaces. This breakage is such that the broken rock has a velocity as it leaves the wall surface. The spalled pieces of rock vary in size and in the velocity with which they leave the wall surface. To provide protection in an underground

opening against the action of flyrock, and in some cases to maintain the opening, the following conditions should be fulfilled:

(1) The compressive stress pulse must not be permitted to enter a protective structure directly so as to cause the same type of fracture in the protective structure as generated on the walls of the tunnel, i.e. spalling fracture caused by reflection of the compressive stress pulse at a free surface.

(2) The interior of the tunnel must be protected from the dynamic load of flyrock of various sizes and velocities.

(3) The accumulated pieces of rock broken from the walls must have some means of support.

Such conditions can best be met by providing a structure within the tunnel that is supported in such a manner that it will not allow direct transmission of a stress pulse into the structure and is strong enough to resist both the impacts of the flyrock and the resulting static load from fractured rock.

2-32 GEOMETRY OF OPENINGS AND PROTECTIVE STRUCTURES. The influence of geometry of an opening on the damage is discussed in EM 1110-345-434. The size and shape of the most effective internal tunnel structure to resist the effects of dynamic loadings might well be considered before the size and shape of a given opening is decided for final design. The factors of use and function dictate the total area required and the minimum dimensions needed, but such factors as the terminal static load and flyrock impacts are influenced by the size and shape of the tunnel, and thus control the design of the protective structure. A balance of these factors for economical design is desirable. It is possible that the size of protective structure for extremely large areas would be far less economical than smaller, longer tunnel arrangements.

The openings should be such that the protective structure can be in the shape of arches or rings, as these are the most effective in withstanding the type of loads that might be imposed. Usually, the protective structure should conform more or less to the tunnel shape. In addition, the stress pulse will be turned away from the protective structure by a mismatching of the mechanical impedance. This mismatching of mechanical impedance is most easily accomplished by leaving a space between structure

and tunnel wall. This space should not be large and need not be more than a few inches.

2-33 AVAILABLE EXPERIMENTAL DATA. No experimental data are available regarding loadings on protective tunnel structures that result from nuclear explosions. Some experimental data and observations of HE explosions have been obtained by the Corps of Engineers on tunnels with no internal structures [6, 7, 8]. One should recognize, therefore, that the loading and response of protective structures in tunnels as presented here are based only on the types of experiences and observations gained from the field work described in these references. Explosive effects from HE bombs are much more localized than would be ground shock directly transmitted through the rock or airblast-induced ground shock from atomic weapons. Therefore, the zoning phenomena, which are described in EM 1110-345-434 and referred to in paragraph 2-44 following, would not be directly applicable when designing protection from large atomic weapons. However, the physical behavior of the bounding material would be similar in many respects and data presented may be possible of extrapolation and adaptation to designing internal structures in rock to resist atomic weapons.

CONVENTIONAL TUNNEL SUPPORTS

2-34 GENERAL CONSIDERATIONS. Linings are used normally for the purpose of maintaining a stable opening from the static viewpoint. The design for static stability may well be coupled with the design for protection against blast loading failure. For this reason the general characteristics of ordinary types of construction are discussed briefly.

2-35 STATIC LOAD CONSIDERATION. Supports in the form of tunnel linings are generally used when the tunnel is in or must pass through an area of defective rock. Here the choice of the type of tunnel support depends on the nature and characteristics of the prevailing rock defects. Such problems of selecting particular types of supporting structures are treated in reference [20]. These structures are usually similar in type, characteristic, and function. They all are composed of transverse ribs, either circular when squeezing or swelling rock is encountered, or beam or arch

ribs supported on posts when the problem is one of supporting a slabbing or collapsing roof. These ribs support longitudinal members over which a lagging is placed. This lagging may be either tight or loose. The completed structure is back-packed with stone, gravel, or concrete, and often the whole structure is concreted in place. A typical lining is composed of ribs, longitudinal members, lagging, packing, and may or may not be concreted. The function is to maintain stability of the opening and prevent rock from dropping to the floor of the tunnel due to slaking and flow fracture. Considerable care is usually taken to see that the ribs and longitudinal members are loaded at multiple points. Struts are often placed across the invert if side pressures are heavy. Ribs in the shape of circles are much preferred when the pressures are more severe.

2-36 DYNAMIC CONSIDERATIONS. The mechanical impedance match is near to unity when static structures are concreted to the wall of the tunnel. In this case one can expect the impinging compressive stress pulse to produce the same type of physical action at the surface of the structure as that which produces failure at the surface of a rock tunnel. Concrete with reinforcing will resist heavy spalling more than plain concrete and more than a bare rock surface.

2-37 APPEARANCE CONSIDERATION. Conventional linings are usually of very light construction in a solid or intact rock condition. What one sees as he passes through a tunnel is not necessarily any indication of the type of construction needed for protection against explosive pulses. The appearance of the inner tunnel lining surface is an important psychological factor. This factor is kept in mind when designing present-day tunnels for public use.

The appearance of the inner face of the liner is important in an opening where personnel are to be housed or subjected to working conditions for hours at a time. The designer should incorporate this factor into his tunnel liner design.

UNDERGROUND DYNAMIC LOADING

2-38 STRESS PULSE. An elastic, isotropic, and homogeneous medium can support the propagation of two types of stress pulses; first, a direct

stress pulse either tension or compression, called a dilatation pulse; and second, a shear stress pulse. The particle motion in a dilatational pulse is parallel to the direction of its propagation, while in the shear pulse the particle motion is perpendicular to the direction of propagation. A dilatation pulse only will be generated from a symmetrical explosion in the interior of an unbounded medium. The explosion in practical cases is not symmetrical and normally occurs relatively close to some surface. Both types of pulses are generated under these conditions and a complex pulse is present. In addition, the surface supports various types of surface waves.

This rather complicated problem is greatly simplified by the fact that the rock as a medium behaves near a free surface in a relatively brittle manner. That is to say, rock exhibits much greater resistance to fracture by the application of compression and shear stresses than it does to tensile stresses. The simplification comes about by the conditions of fracture, which, due to the weakness in tension, means that fracture is produced by small tensile stresses when large shear and compression stresses will not produce failure. Also, when a dilatation pulse strikes a free surface it is reflected with a phase change of 180 degrees; thus, a compression pulse becomes a tensile pulse. Therefore, if the medium is much weaker in tension than in shear, only the dilatation part of the pulse need be considered since fractures at free surfaces, as on the walls of a tunnel, are of primary interest. A rock medium is not perfectly elastic, homogeneous, and isotropic, but full of joints and other types of discontinuities. A consideration of the influence of these discontinuities on the dilatation pulse is necessary. A dilatation pulse impinging upon a boundary between media which have different physical characteristics of density and elasticity will be reflected and refracted under conditions which are not simple. A reflected and refracted pulse of the shear type will be generated as well as a reflected and refracted pulse of the dilatation type.

The intensities of the reflected and refracted pulses depend on the amplitude of the incident disturbance; the angle of incidence; the wave shape of the incident disturbance; the nature, size, and shape of the reflecting surface; the properties of the medium; and the distance from the

boundary to the point considered. The calculations required for the rigorous solution of any reflection problem are extensive and require a detailed knowledge of the properties of the medium. Rigorous treatment will not be attempted here since we are interested essentially in generalizations from tensile reflections. Certain effects will be examined using simplified conditions.

2-39 METHOD OF DETERMINING THE EXTENT OF IMPEDANCE MISMATCHING. Reflection and refraction of waves at the interface of two media are discussed briefly to show the necessity of mismatching the mechanical impedance of any two media which have different physical properties and are bonded together. When an elastic dilatation wave of displacement amplitude A_1 impinges upon an interface, generally four waves are generated as shown in figure 2.16. Waves of displacement amplitude A_4 and A_5 are refracted into the second medium, and waves of displacement amplitude A_2 and A_3 are reflected back into the first medium. Waves A_2 and A_4 are of the dilatation type and waves A_3 and A_5 are of the shear type. Angle α_1 is the incident angle of wave A_1, angles α_2 and α_4 are associated with the reflected and refracted dilatation waves, respectively, and angles β_3 and β_5 are associated with the reflected and refracted shear waves, respectively.

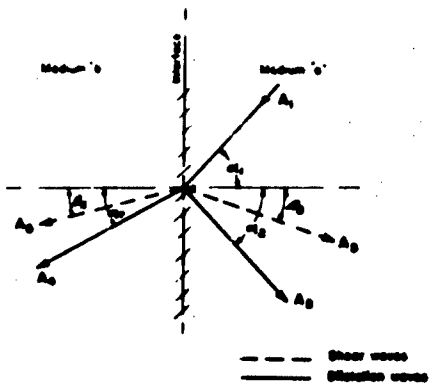

Figure 2.16. Reflection and refraction of an incident dilatation wave at a plane interface

Neglecting the energy of the boundary disturbances, formulas for computing the relative amounts of energy transferred to these four waves have been given by Knott [12]. Formulas for computing the relative amplitudes have been given by Zoeppritz [29], Macelwane [14], and Kolsky [13]. Full derivation and discussion of these formulas can be found in any standard textbook on seismology.

There are four seperate boundary conditions at the interface. These boundary conditions are satisfied if it is assumed that Huygen's

principle can be applied to these waves. This leads to the relations:

$$\frac{\sin \alpha_1}{c_a} = \frac{\sin \alpha_2}{c_a} = \frac{\sin \beta_3}{v_a} = \frac{\sin \alpha_4}{c_b} = \frac{\sin \beta_5}{v_b} \qquad (2.27)$$

where c_a and v_a are the velocities of propagation of the dilatation and shear waves in the first medium, and c_b and v_b are the corresponding velocities in the second medium. The velocity, c, of the dilatation wave in any medium can be computed from the relation

$$c = \left[\frac{E(1 - \mu)}{(1 + \mu)(1 - 2\mu)\rho}\right]^{1/2} \qquad (2.28)$$

and the velocity, v, of the shear wave in any medium can be obtained from the relation

$$v = \left[\frac{E}{2(1 + \mu)\rho}\right]^{1/2} \qquad (2.29)$$

The modulus of elasticity in tension, E, Poisson's ratio, μ, and the density of the medium, ρ, are readily available from a physical properties analysis of the particular medium.

Utilizing the proper boundary conditions, it can be shown that the following four relations between amplitudes are valid:

$$(A_1 - A_2) \cos \alpha_1 + A_3 \sin \beta_3 - A_4 \cos \alpha_4 - A_5 \sin \beta_5 = 0 \qquad (2.30)$$

$$(A_1 + A_2) \sin \alpha_1 + A_3 \cos \beta_3 - A_4 \sin \alpha_4 + A_5 \cos \beta_5 = 0 \qquad (2.31)$$

$$(A_1 + A_2) c_a \cos 2\beta_3 - A_3 v_a \sin 2\beta_3 - A_4 c_b (\rho_b/\rho_a) \cos 2\beta_5 - A_5 v_b (\rho_b/\rho_a) \sin 2\beta_5 = 0 \qquad (2.32)$$

$$\rho_a v_a^2 \left[(A_1 - A_2) \sin 2\alpha_1 - A_3 (c_a/v_a) \cos 2\beta_3\right] - \rho_b v_b^2 \left[A_4 (c_a/c_b) \sin 2\alpha_4 - A_5 (c_a/v_b) \cos 2\beta_5\right] = 0 \qquad (2.33)$$

when ρ_a and ρ_b are the densities of the two media.

By substitution in equation (2.27), the four simultaneous equations (2.30), (2.31), (2.32), and (2.33) may be solved to give the amplitudes of the reflected and refracted pulses in terms of A_1, the amplitude of the incident dilatation pulse.

The effect of the mechanical impedance mismatch of any two media which are bonded may be determined. The above considerations define a method for treating the very general case where a dilatational pulse is impinged at some incident angle to an interface between any two media. Referring to the walls of a tunnel, it is true that the explosive pulse will generally fall into this general case. However, the energy distribution is rather complex and the evaluation of all the factors involved is not practical. Since the damage of greatest interest occurs when a pulse impinges at normal incidence to a free surface, the following simplifications of the general case are discussed: (a) a dilatation pulse impinging at normal incidence to an interface between any two media considered to be integrally bonded, and (b) a dilatation pulse impinging at normal incidence to a free surface boundary.

2-40 NORMAL INCIDENCE--TWO MEDIA. Because of normal incidence, angle α_1 is zero, and from equation (2.27) all other angles are zero too. Substituting equation (2.27) into the four equations (2.30), (2.31), (2.32), and (2.33) shows that waves A_3 and A_5 vanish so that only dilatation pulses are generated. The solutions for the ratios between displacement amplitudes A_2/A_1 and A_4/A_1 are then found as:

$$\frac{A_2}{A_1} = \frac{\rho_b c_b - \rho_a c_a}{\rho_a c_a + \rho_b c_b} \qquad (2.34)$$

and

$$\frac{A_4}{A_1} = \frac{2\rho_a c_a}{\rho_b c_b + \rho_a c_a} \qquad (2.35)$$

Equations (2.34) and (2.35) will provide relative displacement amplitudes of the reflected and refracted dilatation pulses A_2 and A_4 as compared to the incident pulse A_1.

The value of the amplitude of the normal stress just before a wave strikes a boundary at normal incidence is:

$$\sigma_n = 2\pi f A_1 c_a \rho_a \tag{2.36}$$

where f is the frequency of the wave.

The values of σ_{na}, the normal stress in medium a, and σ_{nb}, the normal stress in medium b, after the wave σ_n has reacted with the boundary are given by:

$$\sigma_{na} = 2\pi f (A_1 + A_2) c_a \rho_a \tag{2.37}$$

$$\sigma_{nb} = 2\pi f A_4 c_b \rho_b \tag{2.38}$$

These equations apply to all harmonic waves of any frequency and therefore will apply for pulses of arbitrary shape.

The condition that the boundary is bonded requires $\sigma_{na} = \sigma_{nb}$, thus

$$\frac{\sigma_{nb}}{\sigma_n} = \frac{A_4 c_b \rho_b}{A_1 c_a \rho_a} \tag{2.39}$$

or, from equation (2.35),

$$\frac{\sigma_{nb}}{\sigma_n} = \frac{2\rho_b c_b}{\rho_a c_a + \rho_b c_b} \tag{2.40}$$

Equation (2.34) shows that the amplitude of the reflected wave depends on the quantity $(\rho_b c_b - \rho_a c_a)$ and no wave will be reflected at normal incidence when the product of the density and velocity is the same for the two media. This product "ρc" is referred to herein as the "mechanical impedance" of the medium. Equation (2.34) also shows that when the mechanical impedance of the second medium (medium b) is greater than that of the first (medium a), the amplitude of the displacement on reflection is of the same sign as that of the incident wave. The amplitude changes in sign when the mechanical impedance of the second medium is lower than that of the first, and there is a change in phase on reflection. A compressive stress pulse of sufficiently large amplitude traveling in a medium and impinging

at normal incidence upon a free surface may cause a tensile fracture. A dilatational and a shear pulse are produced when a compression pulse impinges at other than normal incidence. The interference of such reflected pulses gives rise to very complicated stress distributions and the superposition of several reflected pulses may produce tensile stresses which are sufficiently large to cause fracture.

2-41 ILLUSTRATIVE EXAMPLE. The importance of impedance mismatching can be demonstrated best by the following numerical examples considered for normal incidence of the pulse and assuming the media are well bonded.

Physical properties for sandstone, granite, concrete, and a sand cushion material for this example are as follows:

Material	Young's Modulus (E), psi	Poisson's Ratio (μ)	Weight Density (w) lb/cu ft	Mass Density $\left(\rho = \frac{w}{g}\right)$, $\frac{\text{lb-sec}^2}{\text{ft}^4}$	Long Velocity (c), fps	Mechanical Impedance (ρc), $\frac{\text{lb-sec}}{\text{cu ft}}$
Sandstone	2.8×10^6	0.44	140	4.35	17.3×10^3	0.75×10^5
Granite	5.6×10^6	0.25	168	5.22	13.6×10^3	0.71×10^5
Concrete	3×10^6	0.10	150	4.76	9.7×10^3	0.45×10^5
Sand cushion	1×10^3	0.20	150	4.76	0.185×10^3	0.009×10^5

Consider the case of the wave passing from the sandstone medium through the interface into the concrete medium. The ratio of mechanical impedance of concrete to that of sandstone $\rho_c c_c / \rho_{ss} c_{ss}$ is $0.45 \times 10^5 / 0.75 \times 10^5 = 0.60$, and the ratio of stress in the concrete to that in the sandstone from equation (2.40) is:

$$\frac{\sigma_c}{\sigma_{ss}} = \frac{2\rho_c c_c}{\rho_{ss} c_{ss} + \rho_c c_c} = \frac{2 \times 0.45 \times 10^5}{(0.75 + 0.45) \times 10^5} = 0.75$$

Next, consider the case of the wave passing from granite to concrete. The ratio of mechanical impedance of concrete to granite $\rho_c c_c / \rho_g c_g$ is $0.45 \times 10^5 / 0.71 \times 10^5 = 0.63$, and from equation (2.40) the ratio of stress in concrete to granite σ_c / σ_g is $0.9/1.16 = 0.78$. Thus, the stress in the concrete is not reduced substantially and the stress pulse in the medium is well coupled to the concrete.

Next, assume that a layer of sand cushion is placed between a rock

wall and a concrete liner. The mechanical impedance ratio for sand cushion to sandstone $\rho_{sc}c_{sc}/\rho_{ss}c_{ss}$ is $0.009 \times 10^5/0.75 \times 10^5 = 0.012$, and to granite $\rho_{sc}c_{sc}/\rho_g c_g$ is $0.009 \times 10^5/0.71 \times 10^5 = 0.013$. The stress ratio for the sandstone case from equation (2.40) is $0.018/0.759 = 0.024$, and for granite is $0.018/0.719 = 0.025$.

The pulse in passing through the sand cushion is considerably reduced in intensity. Consider the stress in the liner for these last two cases in terms of the stress in the original medium. From sandstone to sand cushion to concrete liner,

$$\sigma_c/\sigma_{ss} = 0.024 \times \frac{2 \times 0.45}{0.459} = 0.047$$

and from granite to sand cushion to concrete liner,

$$\sigma_c/\sigma_g = 0.025 \times \frac{2 \times 0.45}{0.459} = 0.049$$

Thus, the stresses have been reduced to about 5 percent of that in the original medium.

2-42 FREE SURFACE INTERFACE. A free surface, such as in a tunnel, provides near zero impedance matching at the boundary. Only two pulses of importance, a shear pulse and a dilatation pulse, are generated and reflected when a compressional pulse strikes a free surface. Nearly all the incident energy is reflected in the dilatation pulse which is now a tensile stress pulse.

The angle of reflection of the shear pulse is given by [6]

$$\frac{\sin \alpha_1}{\sin \beta_3} = \frac{c_a}{v_a} = \left[\frac{2(1-\mu)}{(1-2\mu)}\right]^{1/2} \qquad (2.41)$$

where

α_1 = the angle of incidence
β_3 = the angle of reflection of the shear wave
c_a = the propagation velocity of the dilatation wave
v_a = the propagation velocity of the shear wave
μ = Poisson's ratio

The angle of reflection of the dilatation pulse is equal to the angle of incidence.

Assuming that the refracted pulse amplitudes at the free boundary are zero, the following formulas give the relative amplitudes of the reflected dilatation and shear pulses in terms of the amplitude of the incident dilatation pulse at a free plane boundary [6].

$$\frac{A_2}{A_1} = \frac{\sin 2\alpha_1 \sin 2\beta_3 - \left(\frac{c_a}{v_a}\right)^2 \cos^2 2\beta_3}{\sin 2\alpha_1 \sin 2\beta_3 + \left(\frac{c_a}{v_a}\right)^2 \cos^2 2\beta_3} \tag{2.42}$$

$$\frac{A_3}{A_1} = \frac{2\left(\frac{c_a}{v_a}\right) \sin 2\alpha_1 \cos 2\beta_3}{\sin 2\alpha_1 \sin 2\beta_3 + \left(\frac{c_a}{v_a}\right)^2 \cos^2 2\beta_3} \tag{2.43}$$

These equations apply to all harmonic waves of any frequency and therefore will apply for pulses of arbitrary shape. In equations (2.42) and (2.43), A_1 is the displacement amplitude of the incident dilatation pulse, A_2 is the displacement amplitude of the reflected dilatation pulse, A_3 is the displacement amplitude of the reflected shear pulse, and the other symbols are as previously defined.

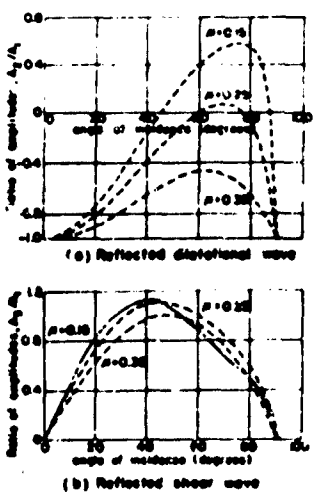

Figure 2.17. Reflected amplitudes for plane dilatation wave incident at free surface

Figure 2.17 indicates the result of plotting A_2/A_1 versus the angle of incidence for a Poisson's ratio of 0.15, 0.25, and 0.35. Take the case where $\mu = 0.35$ as an example; the graph shows that the amplitude of the reflected shear wave is a maximum at an angle of incidence of about 48 degrees. Its amplitude is then a little greater than that of the incident wave. The amplitude of the reflected dilatation wave is a minimum at an angle of incidence of about

65 degrees. At grazing incidence no distortion pulse is reflected and A_2/A_1 again becomes unity.

Relatively large amplitudes of the shear wave are reflected for angles of incidence between 15 and 75 degrees. For angles of incidence between 50 and 80 degrees, the reflected dilatation wave has a relatively small amplitude; for low values of Poisson's ratio in this range of incident angles, the reflected longitudinal wave is in phase with the incident dilatation wave, that is, an incident compressive pulse is reflected as a compressive pulse and a shear pulse. The energy of the initial dilatation wave at the boundary is distributed between the reflected dilatation and shear waves, and is given by:

energy of initial dilatation wave = energy of reflected dilatation + energy of reflected shear

or, in terms of amplitudes and angles of reflection this may be written as

$$1 = \frac{A_2^2}{A_1^2} + \frac{A_3^2 \sin 2\beta_3}{A_1^2 \sin 2\alpha_1} \qquad (2.44)$$

The energy density of a shear wave is less than that of a dilatation wave of the same displacement amplitude, since the ratio of $\sin 2\beta_3/\sin 2\alpha_1$ is always less than unity. This is further substantiated by the fact that the shear wave is reflected at an angle less than the reflected dilatation wave angle, which requires that the width of the reflected beam of the shear wave will be greater than the width of the reflected dilatation beam. Hence, the energy density for the shear pulse must be lower on reflection for equal displacement amplitudes than the dilatation pulse. Equation (2.44) applied to the amplitude functions shown in figure 2.17 indicates that the conservation of energy has been maintained.

Figure 2.18 illustrates the stress distribution at various stages when a plane compressional pulse of triangular shape is reflected at right angles to a free surface. The resultant stress, indicated by heavy solid lines, at any point during reflection is obtained by adding the stresses due to the incident and reflected pulses which are shown by the thin lines in each figure, while the broken line corresponds to the portion of the

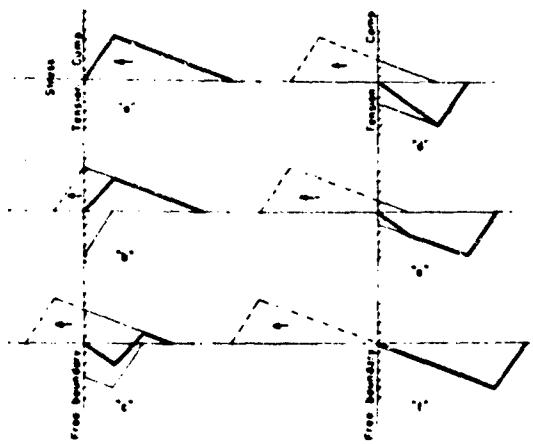

Figure 2.18. The tensile reflection of triangular compression pulse at normal incidence to a free boundary

pulse which has already been reflected. Figure 2.18a shows the pulse approaching the free boundary, figure 2.18b shows the distribution when a part of the pulse has been reflected but the stress still consists entirely of compression, figure 2.18c is a slightly later stage when some tension has been set up near the boundary, and in figures 2.18d and 2.18e this tension has spread and the stress is entirely in the form of tension. In figure 2.18f the reflection is completed and the tension pulse is of the same shape as the incident compression pulse.

As can be seen in figure 2.18, appreciable tension will first be set up at some distance from the free surface and it is here that fractures will begin. Once a fracture has started, the rest of the pulse is reflected at the new free surface formed, so that a series of approximately parallel cracks may be produced when the amplitude of the stress pulse is sufficiently great. Each time a fracture is formed a certain amount of forward momentum is trapped between the fracture and the new free surface. If the fracture extends sufficiently for a piece to be broken off, it will fly off with the momentum trapped in it. This fracturing process may continue such that a series of pieces follow each other in flying off the successive free surfaces. The fracturing process is limited to that region where the resultant tensile stress exceeds the tensile strength of the rock.

2-43 LABORATORY VERIFICATION AND APPROXIMATED FRACTURE PHENOMENA. The fracture of brittle materials by reflected tensile stress is frequently observed in the laboratory. In recent work [21], Rinehart has been able to explain quantitatively, on the basis of reflected tensile stress, the scabbing of a surface of a metal plate by the detonation of an explosive charge against the opposite face of the plate. According to Rinehart,

the number of layers, n, formed in the scabbing process is the first integer smaller than the ratio σ_o/σ_m, where σ_o is the peak compressive stress of the incident wave, and σ_m is the tensile strength of the metal. The thickness of the layers depends on the shape and length of the falling part of the incident pulse. Where the stress curve falls steeply, thin scabs will be formed; as the slope of the stress distance curve decreases, the thickness of the scabs increases. The total thickness of the scabbing is one-half the distance in which the compressive stress of the incident pulse falls from σ_o to $\sigma_o - n\sigma_m$. Rinehart calculates stress from the relation $\sigma = \rho c v$, where σ is the stress, ρ the mass density, c the seismic velocity, and v the particle velocity, and develops a relation between the particle velocity and the velocity of ejection of a pellet. This mechanism, used to explain the scabbing of metal, may be used to explain the type of damage to rock in the recent underground explosion tests [6]. The two phenomena are much the same. The assumptions that the stress wave is plane and is not attenuated appreciably over a distance equal to half the pulse length, and that the material is uniform, probably do not hold so closely for the work with rock as for Rinehart's work with metal.

Consider a saw-tooth pulse in compression with an abrupt rise wave front impinging against a free surface as in figure 2.19a. When this pulse strikes the plane free surface and is reflected, tension is formed immediately. After the reflected pulse has traveled a distance $L/2k$, shown in figure 2.19b, the first spall will occur. The heavy line shows the resultant stress pulse, while the dotted line shows the oncoming compression pulse and the reflected tension pulse. The static tensile strength of the rock is σ_t,

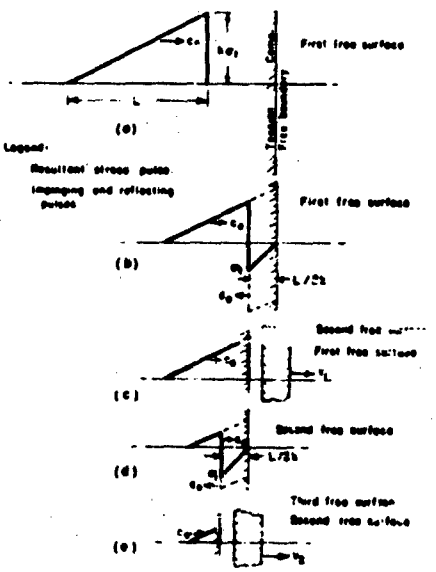

Figure 2.19. Spalling process due to a saw-tooth compression pulse at normal incidence to a free boundary

and L is the pulse length. After the first break, the spalled rock moves away with velocity v_1 and a second free surface is formed with the remaining part of the compression pulse acting upon it, as shown in figure 2.19c. Again upon reflection tension is formed, and when the reflected pulse has traveled a distance L/2k another break will occur if $(k\sigma_t - \sigma_t) > \sigma_t$, i.e. if $k \geq 2$. This is illustrated in figure 2.19d. The second spall moves away with velocity v_2, and a third free surface is formed as indicated in figure 2.19e. This process will continue n times until $(k\sigma_t - n\sigma_t) < \sigma_t$. The important fact is that the rock fractures occurring at a particular location do not occur simultaneously, but in successive stages. Each fracture is separated by a short interval of time. Thus, the tunnel liner is subjected to a series of impacts for a short period of time.

2-44 FALLING AND FLYING ROCK. In the previous section the production of falling and flying rock resulting from the fractures caused by the stress pulse is discussed. The amount, size, and velocities of such fractured rock are discussed in EM 1110-345-434. In that manual four degrees of damage intensity are described and regions of similar damage intensity are denoted as zones of damage. The zone of a given intensity of damage is designated by a number.

The distances from explosion to free surface at which various intensities of damage will occur on various types of rock depend upon the nature of the rock, the size of the explosion, type of explosive, etc. These factors are discussed in EM 1110-345-434.

The zones of damage are briefly described as follows:

Zone 4 damage indicates very light, spotty damage which probably results from dislodging previously broken rock. The geologic structure present determines to a large extent the size of the fractured pieces. For instance, for a tunnel with a long transverse span and in which bedding is nearly horizontal and a few inches apart, fairly large pieces might fall in this zone. If, on the other hand, the tunnel is in rock with bedding steeply inclined to the horizontal or with no bedding, the failures would probably be restricted to the areas where tunnel fractures and cracks were produced in solid rock by the driving process.

Zone 3 indicates moderate continuous damage over the region of the tunnel periphery closest to the explosion. This is a region

where a stress pulse has sufficient amplitude to cause fracture in solid rock. Single or multiple spalls can result in this region. The pieces are not very large as the pulse in this region has just sufficient amplitude to cause single or double spalls. The size of the spalls is not controlled by the rock conditions and strength alone, but also by the shape of the dilatation compression pulse. The shape of the pulse, its length and general slope at pulse front and rear, controls to a large extent the size of the spalled pieces. The general pulse shape encountered in the recent underground explosion tests [6] is approximated by that in figure 2.19. In zone 3, the size and velocity of the rock pieces produced by the pulse are controlled by the geology, rock tensile strength, and pulse shape. In practice one finds that the structural planes of weakness have a large effect upon the size of rock pieces broken free by the pulse. The initial flyrock in zone 3 has a velocity between 2 and 30 fps.

Zone 2 indicates heavy damage continuous over the region of the tunnel periphery closest to the explosion. This is the region where the stress pulse is large enough to cause multiple fractures in solid rock. The size of the pieces of rock is not much larger than the maximum for zone 3 but the maximum initial velocities are probably twice as great; thus, the energy of the rock fragments is about four times as great.

Zone 1 indicates complete breakthrough from the surface. Protection against zone 1 damage is not believed to be feasible; therefore, no further discussion is given.

DESIGN CONSIDERATIONS AND CRITERIA

2-45 DAMAGE PROTECTION. Damage of the type exhibited by zone 4 is similar to the type of failure commonly known as "popping rock" condition. Protection against this kind of damage can be provided by simple means as the flyrock fragments are small and their velocities low. The use of roof bolts would probably be ineffective as the majority of the spalled pieces are only a few inches in size. A screen suspended from the roof that would deflect or hold the spalled or loosened rock and keep it from falling would usually be sufficient. Any light tunnel lining which would bond the surface would be adequate.

Zone 3 protection is not as simple as protection for zone 4 types of damage. Structures are required which will function as follows:

(1) Ensure that isolation from tunnel wall rock is obtained so that the loading pulse is not transmitted directly to the inner tunnel structure.

(2) Provide ability to absorb energy caused by the impact blows from the flyrock.

(3) Provide ability to carry the dead weight of the rock broken from the tunnel.

The distance between the structure and the tunnel wall should be kept as small as possible. This will keep the free-fall velocity of fractured rock to a minimum and reduce the resultant impact loading upon the structure.

Protection against zone 2 type of damage requires an inner tunnel structure somewhat more sturdy than that required by zone 3. As in the previous case, the structure will have to be designed to carry out the same three functions. However, in addition, the structure should provide a mechanism for distributing and softening the impacts of the high-velocity fractured rock, as well as supporting the larger static loads. A material should be placed between the structure and tunnel wall which will not allow direct transmission of the pulse into the structure but will distribute and soften the impacts. Granular materials, such as sand and crushed stone, will be adequate when placed between tunnel wall and structure. This material should completely fill the space and provide a thickness of 5 to 6 in.

2-46 DESIGN LOADS. Tunnel structure design loads for the various intensities of damage for each zone type have been determined from the field tests [7, 8]. The magnitude of the loads to be sustained depends, of course, on the size of the tunnel.

The prediction of design loads depends on the ability to determine the quantity of flyrock or fractured rock and its velocity. It is assumed that the total amount of fragmented rock is independent of the angular position of the region of the tunnel that is subjected to maximum damage. The vertical rock load resting on the structure is variable and will depend upon the angular position of the fragmented section relative to a vertical section through the center line of the tunnel. Figure 2.20 indicates how the structure loading is dependent upon the angular position of the fragmented rock.

The amount of fragmented rock to be used for design purposes is calculated from a consideration of the damage area. The damage area is

the area of the transverse tunnel section (square feet) after blast minus the area of the transverse tunnel section at the same tunnel station before blast [6].

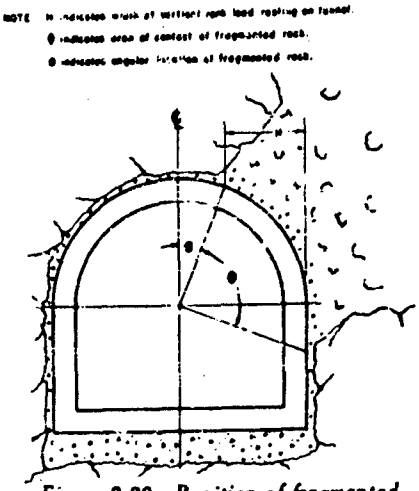

Figure 2.20. Position of fragmented rock on tunnel after explosion

Figure 4.20 in EM 1110-345-434 shows the relation between the scale charge-to-tunnel distance and the tunnel damage area directly under the charge and the zone classification of damage. Additional data pertaining to tunnel damage areas along the length of tunnel is given in table 2-2, page 2-25, of reference [6], a part of which is given in table 2.3. Inspection of these two sets of data allows one to reach the conclusion that for tunnel lining design purposes only, a zone classification of damage is

Table 2.3. Tunnel Damage–Damage Area at Outer Zone Limits

Round	$\bar{r}$ ft	Tunnel Diameter ft	Zone 1A Area sq ft	Zone 2A Area sq ft	Zone 3A Area sq ft	Zone 1B Area sq ft	Zone 2B Area sq ft	Zone 3B Area sq ft
807	6.84	6	20.02	4.01	0.60	20.02	--	--
808	6.84	6	--	3.01	1.00	--	3.37	0.80
809	10.26	6						
810	13.68	6	--	--	1.30	--	--	2.40
811	13.68	6	--	8.80	0.20	--	6.61	1.50
812	13.68	6	--	14.00	1.00	--	12.00	2.51
813	21.55	6	--	11.98	1.50	--	11.00	0.30
814	34.2	15	--	34.97	10.00	--	27.15	8.00
815	34.2	15	360.25	45.03	4.00	450.08	--	--
816	34.2	15	384.81	76.96	4.99	600.03	67.02	--
817	68.4	30	--	371.48	10.15	--	193.22	--

Note: The damage area is the area of the transverse tunnel section (square feet) after blast minus the area of the transverse tunnel section at the same tunnel station before blast; $\bar{r}$ is the characteristic length (feet) numerically equal to the cube root of the charge weight in pounds.

The letter A, included as part of the zone number, refers to the damage zone toward the tunnel portal and B to the zone toward the tunnel face.

justified because of the large spread in the observed damage areas under the various experimental conditions. Also, the variables of each tunnel site, and the range of weapons that may be used against it for damage, are so great that any attempt to predict the possible extent of damage closer than a zone classification cannot be justified.

Average values of the expected percent damage areas for the various zones can be obtained as follows. Table 2.3 shows that the average damage area for the outer limit of zone 3 was 1.19 sq ft for the 6-ft-diameter tunnels. This value multiplied by 100 and divided by the original transverse area gives 4.2 percent damage area. A similar computation for the 15-ft-diameter tunnel gives 3.8 percent damage area. Likewise, computations for zone 2 outer limit yield for the 6-ft tunnel 29.4 percent damage area, and for the 15-ft tunnel, 28.5 percent damage area. It should be noted that the percent damage area in zone 2 becomes very large as zone 1 is approached. Designing tunnel linings for protection against more than an 80 percent damage area does not appear practical; therefore, this value is arbitrarily selected as the upper limit of zone 2.

For design purposes the percent damage area at the upper limit of zone 4 and the lower limit of zone 3 is arbitrarily rounded off at 5 percent; likewise, the percent damage area at the upper limit of zone 3 and the lower limit of zone 2 is rounded off at 30 percent, also the upper limit of zone 2 is set at 80 percent. The expected scale charge-to-tunnel distances for these various percent damage areas can be obtained from figure 4.20 and are summarized in table 2.4.

The magnitude of the maximum velocity of the fractured rock varies

Table 2.4. Probable Percent Damage Area of Each Zone

Zone	Scale Distance	Percent Damaged Area
4	6.0	0-5
3	4.0	5-30
2	2.5	30-80
1	-	breakthrough

from zone to zone and within each zone. However, the velocities of the first pieces to fracture at any point in a particular zone are much greater than the velocities of the last pieces to fracture during the period of damage. Probably the last pieces to fracture have little if any initial velocity. Table 2.5 is a listing of the probable maximum velocities for spalled rock in the various zones as obtained from EM 1110-345-434.

Table 2.5. Probable Maximum Velocities of Spalled Rock

Zone	Scale Distance	Velocity Range, fps
4	6.0	0-2
3	4.0	2-30
2	2.5	30-60

For design purposes, the impacts which the inner tunnel structure receives should be considered as successive impacts. The first impacts are derived from small fragments at high velocities, and the last impacts are associated with relatively larger pieces at relatively lower velocities. Therefore, the energy per impact is some fraction of the total energy. The total energy can be calculated by using the total mass of the rock broken per foot of tunnel associated with a velocity of half the maximum velocity for that zone. The fraction of the total energy per impact recommended for design purposes is for zone 2, 1/10, for zone 3, 1/5, and for zone 4, 1/2. There is no experimental data available for the dynamic loading of inner tunnel structures resulting from underground explosions. The above recommendations are based on field data and observations resulting from the experiments of the Corps of Engineers [1], in particular, high-speed motion pictures, Rinehart's theory of fracture, and the approximated phenomena of fracture (paragraph 2-43). Probably most of the energy is dissipated from each impact before the next impact occurs. This is held possible since the time difference is great enough between each impact. The high-speed movies indicated that the fracture phenomena were spread over a large number of frames at a speed of 400-800 frames per second, and thus justify a time dissipation of energy.

2-47 TERMINAL STATIC LOAD. The final static load resting upon the internal tunnel structure depends upon the quantity of rock broken free from the tunnel wall surface, and the distribution of this broken rock around the periphery of the liner. The damage will vary for any given explosion, and depends primarily on the distance of each point of the tunnel with respect to the explosion. This damage is characterized by the designation of zones explained previously. In any design for protection, a selection of the maximum protection desired for the whole tunnel would need to be made, such as protection against zone 3 loading, etc. The quantity of rock fractured per foot of tunnel can be determined [6] by utilizing the information given in table 2.4.

The angular location of the explosion and the distance between the tunnel lining and the wall surface determine what portion of the fractured rock will need to be supported by the tunnel. The broken rock will distribute somewhat uniformly over the upper region of the lining when the explosion is directly overhead. Most of the broken rock will support itself if the explosion occurs directly out from the equatorial radius. If the initial distance between the inner tunnel structure and the tunnel wall surface is small, or if a crushed stone cushion is used between this protective structure and the tunnel wall, most of the broken rock will remain in place no matter where the explosion is angularly located. If a large open space is left between the protective structure and the tunnel wall, then broken rock will slide off the lining and build up around the lining from the bottom. From the static design viewpoint each position of damage needs to be examined separately. Keeping the distance between the internal tunnel structure and the tunnel wall small will reduce the terminal static loading by utilizing wedging and arching action of the broken rock. It is easier to prevent rock motion than to stop it.

2-48 ADEQUACY OF CONTACT LINERS. As stated before, one of the main functions of a structure or liner for protection against underground explosive loads is to provide as close to a zero mechanical impedance match as possible. While an open space provides nearly a perfect mismatch, it allows other types of loads to be greater than need be. This mismatching of the mechanical impedance can be carried to a high degree by placing any

kind of material that has a lower density than the rock medium between the tunnel liner and the tunnel wall. A granular material with a high percentage of voids is particularly effective. If any present type liner is insulated from the tunnel wall by such material, and is strong enough to carry the static load resulting from the explosive shock, it could well be called a good protective liner. However, a major point of importance is that liner foundations should also be cushioned from the solid rock by a granular material such as a sand and crushed stone layer. This is essential to minimize the transmission of the pulse to the liner by way of the foundation, and to absorb any impact vibrations that may exist.

2-49 SELECTING ADEQUATE PROTECTIVE LINERS. The liner required for adequate protection will depend upon the type of rock, the depth of the tunnel, the function of the tunnel, and the kind of weapons which would be used against the tunnel. Under one set of conditions a tunnel might require no liner for protection against bombings, while the same tunnel under another set of conditions would require liner protection. The limits of anticipated damage can be obtained by applying the principles set down in EM 1110-345-434. It is obvious that if any underground installation is subjected to atomic bomb attack and the bomb can bring about damage as in zone 1 with a breakthrough occurring, the whole tunnel in that region between the blast doors will become completely contaminated. Therefore, the minimum depth for adequate protection must be greater than the distance to effect a zone 1 type of damage. Whether or not it would be more practical in each case to go deeper or to provide protection against zone 2 type of damage depends on the actual situations met in each case.

2-50 DETERMINATION OF DESIGN LOADS. The design loads are ascertained after the intensity of the type of damage is established for which protection is desired. The design procedure for each case of zone 4 type through zone 2 type of damage protection may be slightly varied. It may be possible, for instance, for a single liner to provide all the necessary protection even where the basic rock is of such a nature that artificial supports are necessary to maintain a statically stable opening, and where protection is also necessary against explosive loads. Thus, a single liner can serve two basic functions. This might be carried out by simply

providing a layer of granular material between the liner and the walls and roof of the tunnel.

Figures 2.21, 2.22, and 2.23 indicate some ideas of what may be done to meet varying conditions. The designer can vary the construction to meet

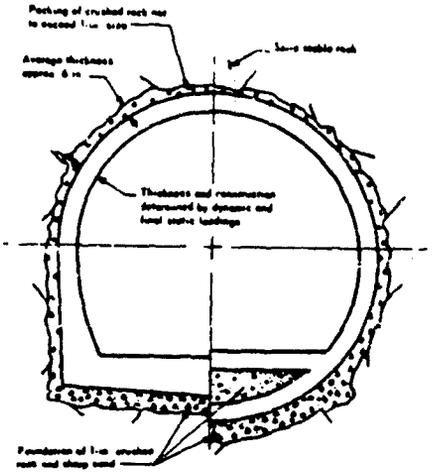

Figure 2.21. Typical internal structure--horseshoe or circular shape--for zones 2 and 3

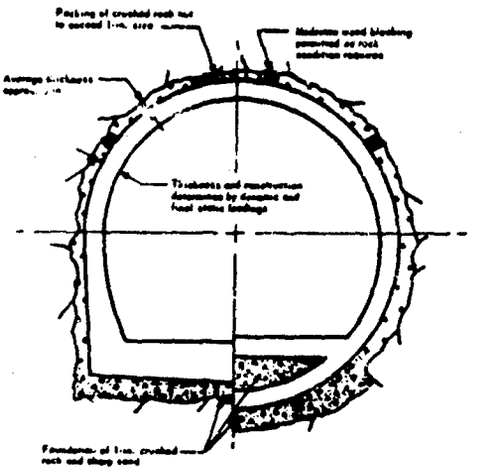

Figure 2.22. Typical internal structure--horseshoe or circular shape--for zones 2 and 3

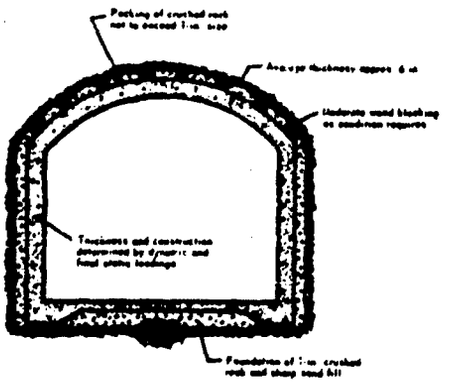

Figure 2.23. Typical internal structure--flat arch--for zones 2 and 3

the particular conditions adhering only to the principles set forth in this manual.

After the size of opening is set and the degree of damage protection determined, the loads are evaluated as set forth herein. EM 1110-345-434, figure 4.22, establishes a correction factor to be used for tunnels where the tunnel scale diameter is greater than 0.44. This correction factor multiplied by the predicted damage area as set forth in figure 4.20 gives values in agreement with experimental observations. This correction factor may be applied in the same way to the values given in table 2.4.

The following example is given to illustrate the use of the design principles in order to determine the design loads, both static and dynamic, and to determine a value of wall thickness for a reinforced concrete structure. An average value of 3 in.-lb per cu in. for reinforced concrete has been assumed as the energy absorption factor. This factor will vary depending upon the type of construction material used and the size and shape of the structure. Therefore, the energy absorption factor should be determined for each installation.

2-51 ILLUSTRATIVE EXAMPLE. Assume that a tunnel of the type shown in figure 2.20 is to be designed and built to provide protection from bombing attacks. The specific use of this tunnel requires that protection be provided for expected zone 3 type damage as caused by a bomb containing 25,000 lb of explosive. Assume that the tunnel is located in rock and at a depth such that it will be subjected to this type of damage. Assume that the bomb detonates directly over the tunnel such that the maximum weight of spalled rock rests upon the full width of the tunnel lining.

The tunnel is to have approximately the following dimensions: width (or diameter), 12 ft; height to spring line, 6 ft; radius of circular roof, 6 ft.

The scale diameter is given by

$$T/W^{1/3} = 12/(25{,}000)^{1/3} = 0.41 < 0.44$$

Since the scale diameter is less than 0.44 no correction factor need be applied to the damage values and the percent damage area can be read directly from table 2.4 as ranging from 5 to 30 percent. For maximum protection the 30 percent value will be used. The damaged area expected is

$$0.30 \times \text{the transverse area} = 0.30\left[\frac{1}{2} \times \frac{\pi(12)^2}{4} + 12 \times 6\right] = 38.6 \text{ sq ft}$$

The total weight of fractured rock is

$$38.6 \text{ sq ft} \times 130 \text{ lb/cu ft} = 5018 \text{ lb/ft of tunnel length}$$

From paragraph 2-46 for zone 3 type damage, the energy per impact factor is 1/5 of the total energy of the total mass of rock broken per foot of tunnel length. Therefore, for impact design the weight of rock per impact is

$$1/5 \times 5018 = 1004 \text{ lb/ft of tunnel}$$

From table 2.5 the velocity range of fractured rock is from 2 to 30 fps. Again from paragraph 2-46, half the maximum velocity is used, therefore, $v = 30/2 = 15$ fps.

So, the energy per impact per foot of tunnel is

$$1/2 \times \text{mass} \times v^2 = 1/2 \times (\text{weight/gravity}) \times (\text{velocity})^2$$
$$= 1/2 \times (1004/32.2) \times 15 \times 15 = 3508 \text{ ft-lb}$$

Now permitting a factor of absorption of 3 in.-lb per cu in. for reinforced concrete, the thickness of a concrete lining can be calculated. The energy of allowable absorption must equal the energy placed upon the structure. So for one foot of length of lining the permitted absorption is approximately

$$\left[\frac{1}{2} \times \pi \times \text{diameter (ft)} + (2 \times \text{spring-line height (ft)} + \text{width (ft)}\right]$$
$$\times \text{thickness } (t) \times 3 \text{ in.-lb/cu in.} \times 144 \text{ sq in./sq ft}$$
$$= \left[\frac{1}{2} \times \pi \times 12 + (2 \times 6) + 12\right] \times t \times 432 \frac{\text{(ft-lb)}}{\text{cu in.}}$$
$$= (6\pi + 24)\ 432t = 18{,}511t \text{ ft-lb/ft}$$

This factor is equal to the energy per foot of tunnel per impact, and the lining thickness is

$$t = \frac{3{,}508}{18{,}511} = 0.1895 \text{ ft} = 2.27 \text{ in.}$$

For static considerations, after the rock has settled at rest, and assuming the worst condition where the total weight of the broken rock rests upon the tunnel lining, the static design would use the above

calculated value of 5018 lb per foot of tunnel length, or

$$\frac{5018}{12} = 418 \text{ lb/ft of tunnel width}$$

It appears that dynamic considerations in the design of the protective lining for this particular tunnel can be eliminated. Any thickness greater than t = 0.1895 ft will provide the necessary dynamic protection, and a greater thickness than this is generally necessary to even build such a structure. From various handbooks on tunnel lining design [7] tables are available from which the static design can be completed when the load per foot of tunnel length is given. Tables 1 and 2 of reference [7] show clearly in this example that the static load is very small and a minimum design is all that is needed.

Table 2.6 is included to give some examples of computed static and dynamic design loads for zones 4, 3, and 2 on a 9-ft-, 12-ft-, and 15-ft-diameter opening.

Table 2.6. Static and Dynamic Design Loads for 9-ft-, 12-ft-, and 15-ft-Diameter Tunnels of Assumed Circular Cross Section

Zone	Max Damage Area, %	Damage Area, sq ft			Wt of Broken Rock lb/ft of Tunnel		
		Tunnel Diameter, ft			Tunnel Diameter, ft		
		9	12	15	9	12	15
4	5	3.2	5.7	8.8	420	740	1,200
3	30	19.0	34.0	53.0	2500	4,400	6,900
2	80	51.0	90.0	140.0	6600	12,000	18,000
Zone	Impact Factor	lb/ft of Tunnel per Impact			Energy per Impact per ft of Tunnel, ft-lb		
		Tunnel Diameter, ft			Tunnel Diameter, ft		
		9	12	15	9	12	15
4	1/2	210	370	600	3.3	5.7	9.3
3	1/5	500	880	1400	1700	3,100	4,900
2	1/10	660	1200	1800	9200	17,000	25,000

2-52 NATURE OF LINER. The shape and size of the opening for functional purposes and the type of rock and failures anticipated will determine the design features of the inner tunnel structure or liner. The depth of tunnel from bomb penetration viewpoint determines the kind of foundation that will be most suitable. For small tunnels, the inner tunnel structure may be as a ring or rigid frame of simple construction that can withstand relatively heavy loads. Under certain conditions some kind of bracing structure might be desirable from an economic viewpoint for large openings. As an example, if a multistory building were to be placed in a large opening, an inner structure for protection might well be a system of rigid frames of the usual building type designed to withstand the dynamic rock loads. Figures 2.21, 2.22, and 2.23 are typical simple unscaled designs consistent with the design principles of this manual and are presented to indicate some of the possibilities of interior and exterior shapes. The designer should vary the shape to provide economical driving of the tunnel as well as to meet the functional purpose of the tunnel for safety and efficient use.

2-53 FOUNDATIONS. The inner tunnel structure should be supported on some type of foundation. In most cases the primary pulse will not strike the foundation directly; i.e., the foundation will be on the opposite side of the tunnel from the explosion. In any event, efforts should be made to isolate the pulse generated in the rock by the explosion from any inner tunnel structure. This can be done by preparing a layer of coarse crushed stone between footings and solid rock. The height to which the foundations can conveniently extend around the periphery without being in line with the explosion depends on the possible penetration depths that might take place. Under certain conditions, such as in a mountain side, an explosion could occur below the floor level of the tunnel. Having the foundation isolated from direct strikes of the explosive pulse may not always be possible.

BIBLIOGRAPHY

1. Bucky, P. B., Use of Models for the Study of Mining Problems. American Institute of Mining and Metallurgical Engineers, Technical Publication 425, February 1931, 28 pp.

2. Bucky, P. B., Application of Principles of Similitude to Design of Mine Workings. American Institute of Mining and Metallurgical Engineers, Technical Publication 529, February 1934, 20 pp. Also in Transactions, American Institute of Mining and Metallurgical Engineers, vol 109, February 1934, pp 25-42.

3. Bucky, P. B., and Taborelli, R. V., Effects of Artificial Support in Longwall Mining as Determined by Barodynamic Experiment. American Institute of Mining and Metallurgical Engineers, Technical Publication 1020, February 1939, 12 pp.

4. Duvall, Wilbur I., Stress Analysis Applied to Underground Mining Problems: Part 1, Stress Analysis Applied to Single Openings. U. S. Bureau of Mines, Report of Investigations, 4192, March 1948, 18 pp.

5. Duvall, Wilbur I., Stress Analysis Applied to Underground Mining Problems: Part 2, Stress Analysis Applied to Multiple Openings and Pillars. U. S. Bureau of Mines, Report of Investigations, 4387, November 1949, 11 pp.

6. Engineering Research Associates, Division of Remington Rand, Inc., "Rock." Underground Explosion Test Program (UNCLASSIFIED), Final Report, vol II, Contract No. DA-04-167-eng-298 for Department of the Army, Corps of Engineers (30 April 1953).

7. Engineering Research Associates, Division of Remington Rand, Inc., "Granite and limestone." Underground Explosion Test Program (UNCLASSIFIED), Technical Report No. 4, vol II, Contract No. DA-04-167-eng-298 for Department of the Army, Corps of Engineers (30 August 1952).

8. Engineering Research Associates, Division of Remington Rand, Inc., "Sandstone." Underground Explosion Test Program (UNCLASSIFIED), Technical Report No. 5, vol II, Contract No. DA-04-167-eng-298 for Department of the Army, Corps of Engineers (15 April 1953).

9. Greenspan, Martin, "Effect of a small hole on the stresses in a uniformly loaded plate." Quarterly of Applied Mathematics, vol 2, No. 1 (April 1944), pp 60-71.

10. Greenwald, H. P., "Physics of subsidence and ground movement in coal mines." Journal of Applied Physics, vol 8, No. 7 (July 1937), pp 462-469.

11. Howland, A. C. J., "Stresses in a plate containing an infinite row of holes." Proceedings, Royal Society of London; Series A, Mathematical and Physical Sciences, vol 148, No. 864 (1 February 1935), pp 471-491.

12. Knott, C. G., "Reflection and refraction of elastic waves, with seismological applications." Philosophical Magazine and Journal of Science, vol 48, No. 290 (July 1899), pp 64-96.

13. Kolsky, Herbert, Stress Waves in Solids. Oxford University Press, New York, N. Y., 1953.

14. Macelwane, James B., "Geodynamics," in Introduction to Theoretical Seismology (John Wiley and Sons, Inc., New York, N. Y., 1936), Part 1, pp 156-169.

15. Merrill, Robert H., Design of Underground Mine Openings, Oil-Shale Mine, Rifle, Colorado. U. S. Bureau of Mines, Report of Investigations, 5089, December 1954, 56 pp.

16. Mindlin, Raymond D., "Stress distribution around a tunnel." Proceedings, American Society of Civil Engineers, vol 65, No. 4 (April 1939), pp 619-642. Also in Transactions, American Society of Civil Engineers, vol 105 (October 1940), pp 1117-1140.

17. Obert, Leonard, and Duvall, Wilbur I., Microseismic Method of Predicting Rock Failure in Underground Mining: Part 1, General Method. U. S. Bureau of Mines, Report of Investigations, 3797, February 1945, 7 pp.

18. Obert, Leonard, Windes, S. L., and Duvall, Wilbur I., Standardized Tests for Determining Physical Properties of Mine Rock. U. S. Bureau of Mines, Report of Investigations, 3891, August 1946, 67 pp.

19. Panek, Louis A., Stresses About Mine Openings in a Homogeneous Body. Edwards Brothers, Inc., Ann Arbor, Mich., 1951. Thesis, Columbia University, 1951.

20. Proctor, Robert V., and White, T. L., Rock Tunneling with Steel Supports. Commercial Shearing and Stamping Co., Youngstown, Ohio, 1946.

21. Rinehart, John S., "Scabbing of metals under explosive attack." Journal of Applied Physics, vol 23, No. 11 (November 1952), pp 1229-1233.

22. Roark, Raymond J., Formulas for Stress and Strain, 3d ed. McGraw-Hill Book Co., Inc., New York, N. Y., 1954.

23. Sinclair, David, and Bucky, P. B., "Photoelasticity and its application to mine-pillar and tunnel problems." Transactions, American Institute of Mining and Metallurgical Engineers (Coal Division), vol 139 (1940), pp 224-252, discussion, pp 252-268.

24. Sugihara, T., and Sesaw. K., "Stress in country rock around a vertical or inclined circular shaft." Journal of the Faculty of Engineering, Tokyo University, vol 20, No. 5 (June 1932).

25. Terzaghi, Karl, and Richart, F. E., Jr., "Stresses in rock about cavities." Geotechnique, vol 3, No. 2 (June 1952), pp 57-90.

26. Timoshenko, Stephan, Theory of Elasticity, 2d ed. McGraw-Hill Book Co., Inc., New York, N. Y., 1951.

27. Windes, S. L., Physical Properties of Mine Rock, Part 1. U. S. Bureau of Mines, Report of Investigations, 4459, March 1949, 79 pp.

28. Windes, S. L., Physical Properties of Mine Rock, Part 2. U. S. Bureau of Mines, Report of Investigations, 4727, September 1950, 37 pp.

29. Zoeppritz, Karl. "Erdbebenwellen, VIIb: Über reflexion und durchgang seismischer wellen durch unstetigkeitsflachen." Akademie de Wissenschaften, Göttingen, Nachrichten, Mathematisch-physikalische klasse, Helft 1 (1919), pp 66-84.

FOR THE CHIEF OF ENGINEERS:

W. P. LEBER
Colonel, Corps of Engineers
Executive